Studies by the U.S. Geological Survey in Alaska, 2000
U.S. Geological Survey Professional Paper 1662

Stratigraphy, Age, and Geochemistry of Tertiary Volcanic Rocks and Associated Synorogenic Deposits, Mount McKinley Quadrangle, Alaska

By Ronald B. Cole[1] *and* Paul W. Layer[2]

Abstract

This chapter reports new field, petrographic, and geochemical data for two Tertiary volcanic units and underlying sedimentary rocks in the southeast corner of the Mount McKinley 1:250,000-scale quadrangle. The volcanic units include the late Paleocene and early Eocene volcanic rocks of Foraker Glacier and the late Eocene and early Oligocene Mount Galen Volcanics. New $^{40}Ar/^{39}Ar$ dating on two samples from the lower part of the volcanic rocks of Foraker Glacier yield ages of 56.9±0.2 and 55.5±0.1 Ma. The volcanic rocks of Foraker Glacier unconformably overlie a 550-m-thick sequence of Late Cretaceous(?) sedimentary rocks that dip steeply north and unconformably overlie Paleozoic metamorphic rocks with a schistosity that dips steeply south. The sedimentary sequence includes a metamorphic-clast cobble-boulder alluvial-fan conglomerate overlain by fluvial and lacustrine conglomerate, sandstone, and mudstone. The coarse grain size and presence of bounding unconformities indicate that these sedimentary rocks fill a contractional basin and record pre-late Paleocene tectonic uplift of the adjacent Paleozoic metamorphic rocks. The overlying volcanic rocks of Foraker Glacier consist of a 200-m-thick interval of basalt and andesite lavas containing interbedded mudstone and volcaniclastic fluvial conglomerate overlain by 1,500 m of rhyolite lava and interbedded pyroclastic-flow deposits. The basalts are slightly depleted in incompatible trace elements (light rare-earth elements, Rb, Th, K) and along with the andesites have high Ba/Ta ratios (464–1,160). The rhyolites are strongly enriched in light rare-earth elements (LREEs), Rb, Th, and K, are depleted in Sr, P, and Ti, and have low Ba/Ta ratios (23–137), all of which indicate a combination of crustal assimilation and fractional crystallization in their petrogenesis.

The Mount Galen Volcanics consists of basalt, andesite, dacite, and rhyolite lavas and dacite and rhyolite tuff and tuff-breccia. New $^{40}Ar/^{39}Ar$ dating of a basaltic andesite flow 46 m above the base of the Mount Galen Volcanics yields an age of 42.8±0.5 Ma. The Mount Galen Volcanics is enriched in Ba, Th, Sr, and LREEs, has high Ba/Ta ratios (446–3,734), and exhibits a distinct paired Nb-Ta-depletion trend, all of which are common characteristics of subduction-related volcanic rocks.

We interpret that the Late Cretaceous(?) sedimentary rocks record uplift and shortening during the final stages of accretion of the Wrangellia composite terrane to southern Alaska. The volcanic rocks of Foraker Glacier represent the final phase of Late Cretaceous and early Tertiary Alaska Range-Talkeetna Mountains magmatism that ended with suturing of the Wrangellia composite terrane. The Foraker Glacier primary basaltic magmas were probably derived from a relatively depleted subcontinental mantle source; the rhyolites were then formed by partial melting of crustal rocks and fractional crystallization. The mantle source may have been a partially depleted remnant mantle wedge formed during earlier Kula Plate subduction beneath southern Alaska. The Mount Galen Volcanics is part of the northern segment of the Eocene and Oligocene Alaska-Aleutian arc that crosscuts older igneous rocks of the region.

Introduction

Periodic magmatism is an integral component in the tectonic history of the central Alaska Range. For example, two regional magmatic belts that overlap in the central Alaska Range include Late Cretaceous and early Tertiary rocks of the Alaska Range-Talkeetna Mountains belt and Eocene and Oligocene rocks of the Alaska-Aleutian belt (fig. 1). Each of these belts is generally interpreted to record magmatism that occurred in response to subduction beneath southern Alaska (Wallace and Engebretson, 1984; Moll-Stalcup, 1994). Whereas research has been done to investigate the plutonic rocks of the central Alaska Range (Reed and Lanphere, 1974; Lanphere and Reed, 1985; Reiners and others, 1996), there has been very little work published on the contemporaneous

[1]Allegheny College, Meadville, Pa.
[2]University of Alaska, Fairbanks.

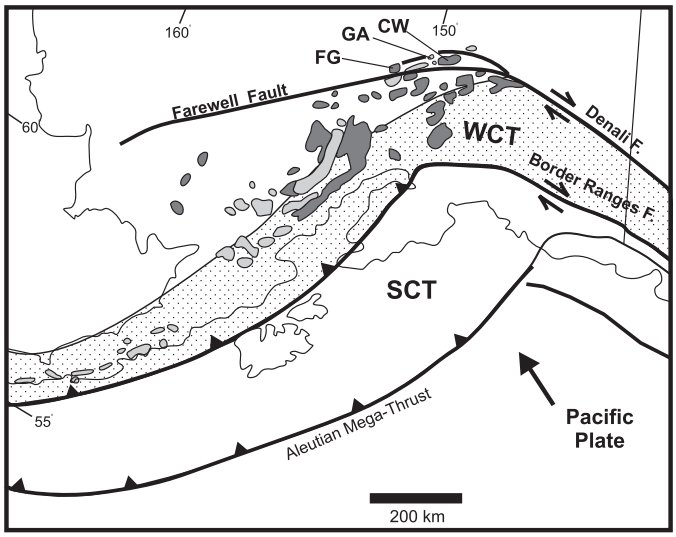

Figure 1. South-central Alaska, showing locations of regional magmatic belts, major faults, accreted-terrane assemblages, and map units: FG, volcanic rocks of Foraker Glacier; GA, Mount Galen Volcanics; CW, Cantwell Formation volcanic rocks; SCT, southern margin composite terrane; WCT, Wrangellia composite terrane (stippled area). Magmatic belts after Moll-Stalcup and others (1994); composite terranes after Nokleberg and others (1994) and Plafker and others (1994).

volcanic rocks (except for Decker and Gilbert, 1978). This chapter presents new stratigraphic, age, and geochemical data, along with a compilation of existing data, for Tertiary volcanic rocks that are exposed in the southern part of the Mount McKinley 1:250,000-scale quadrangle (fig. 2). Our main goals are to present a synthesis of Tertiary volcanism and related sedimentation in the Mount McKinley quadrangle and to provide a regional tectonic context for these events. In a broad sense, these volcanic rocks and underlying synorogenic sedimentary deposits provide a record of pre-late Paleocene tectonic uplift followed by two distinct volcanic episodes along the northwest flank of the ancestral Alaska Range. The first volcanic episode, which occurred during late Paleocene and early Eocene time, closely followed accretion of the Wrangellia composite terrane to southern Alaska (fig. 1). The Wrangellia composite terrane had a prolonged history of accretion to western Canada and southern Alaska extending from Late Jurassic through Late Cretaceous time (Stone and others, 1982; McClelland and others, 1992; Nokleberg and others, 1994). The final phase of accretion of the Wrangellia composite terrane, which is recorded in the study area by deformation in the Cantwell Basin, ended by late Paleocene time (Cole and others, 1999). The second volcanic episode, which occurred largely during early Oligocene time, can be correlated with the subduction-related Alaska-Aleutian magmatic belt.

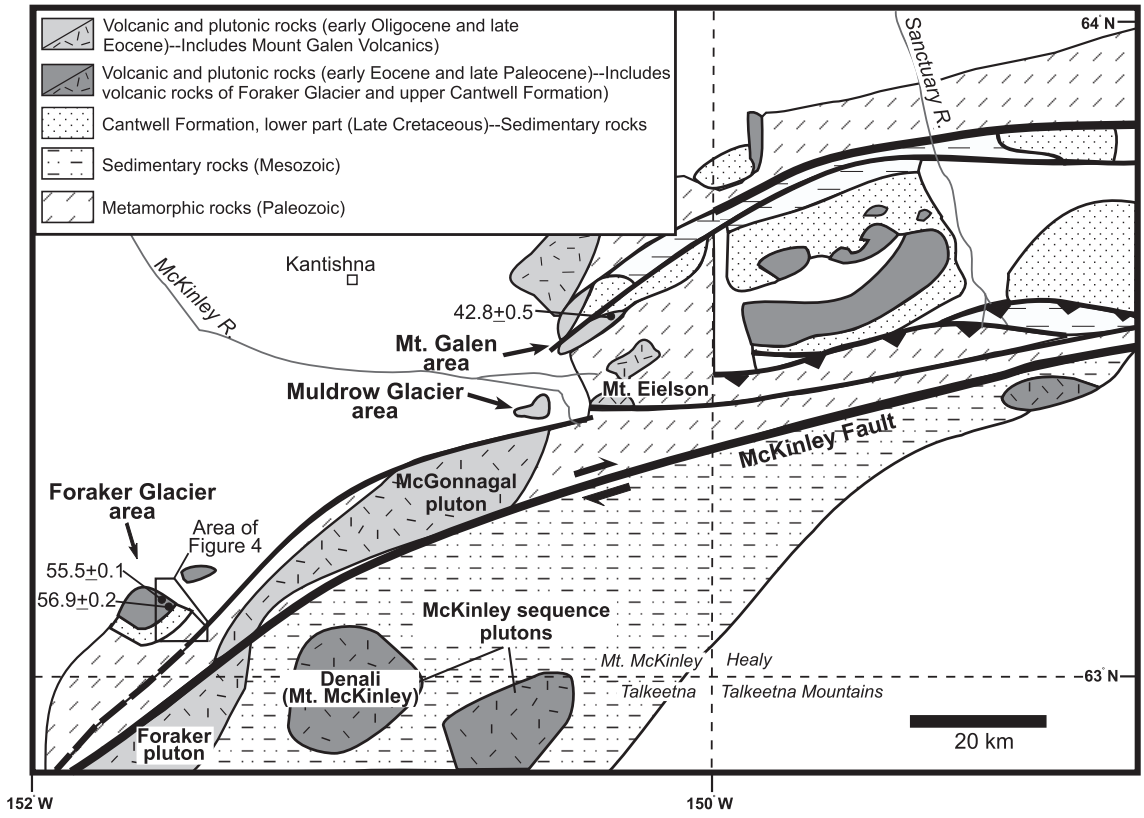

Figure 2. Generalized geologic map of study area in south-central Alaska. Dashed lines denote boundaries of adjacent 1:250,000-scale quadrangles (italic names). Geology from Reed (1961), Reed and Nelson (1980), Csejtey and others (1992), and Wilson and others (1998). Radiometric ages are from this study (table 1).

Ages and Locations of Volcanic-Rock Units

The Tertiary volcanic rocks described in this chapter are exposed in the southern part of the Mount McKinley quadrangle along the east and west sides of Foraker Glacier, the west side of the Muldrow Glacier terminus, and in the vicinity of Mount Galen (fig. 2). All of these rocks were mapped by Reed (1961) as part of the Cretaceous Cantwell Formation. We agree with his mapping that the volcanic rocks of Foraker Glacier are part of the Cantwell Formation, but the age of the Cantwell Formation has since been revised. Ridgway and others (1997) revised the age of the lower part of the Cantwell Formation to Late Cretaceous on the basis of the presence of late Campanian and early Maestrichtian pollen in sedimentary rocks (lithologically equivalent to unit Tcs of Wolfe and Wahrhaftig, 1970). Cole and others (1999) revised the age of the upper part of the Cantwell Formation to late Paleocene and early Eocene on the basis of radiometric ages of volcanic rocks (lithologically equivalent to unit Tcv of Wolfe and Wahrhaftig, 1970). The new $^{40}Ar/^{39}Ar$-plateau ages reported here for the volcanic rocks of Foraker Glacier (fig. 3; table 1) indicate that these rocks are latest Paleocene and early Eocene, coeval with the upper part of the Cantwell Formation at the type area in the Healy quadrangle (Cole and others, 1999).

The volcanic rocks of the Mount Galen area are not part of the Cantwell Formation. These rocks were shown to be late Eocene and early Oligocene and were named the Mount Galen Volcanics by Decker and Gilbert (1978). Published K-Ar ages (Decker and Gilbert, 1978) for the Mount Galen Volcanics (table 1) range from 38.7±1.1 to 41.2±1.2 Ma, with minimum ages of 34.8±1.4 to 39.6±1.2 Ma. The new $^{40}Ar/^{39}Ar$-plateau age of 42.8±0.5 Ma reported here for a basaltic andesite flow 46 m above the base of the Mount Galen Volcanics (sample GA1–46, tables 1–3) more precisely confirms a late Eocene age for the onset of Mount Galen volcanism. On the basis of the K-Ar ages reported by Decker and Gilbert and geochemical correlations of the present study, we concur with Decker and Gilbert that the volcanic rocks of the Muldrow Glacier area correlate with the Mount Galen Volcanics and are part of the late Eocene and early Oligocene group of rocks.

In summary, there are two age groups of volcanic rocks in the study area. The first group, the volcanic rocks of Foraker Glacier, are late Paleocene and early Eocene and occur in the Foraker Glacier area. The second group, the Mount Galen Volcanics, is late Eocene and early Oligocene and is exposed in the vicinity of Mount Galen and along the west side of the Muldrow Glacier terminus.

In addition to the volcanic-rock units of this study, several important plutonic-rock units occur in the study area. Significant late Paleocene and early Eocene plutonic rocks in the region include the McKinley sequence granites, as well as a series of compositionally zoned (peridotite to granite) plutons (Reed, 1961; Reed and Nelson, 1980; Lanphere and Reed, 1985; Reiners and others, 1996). Major plutons of Oligocene age include the Foraker and McGonnagal granites and granodiorites (Reed, 1961; Reed and Lanphere, 1974) and the Mount Eielson granodiorite (Reed, 1933; Decker and Gilbert, 1978). In addition, a poorly exposed fine-grained hornblende granite of unknown age is exposed north of the Mount Galen Volcanics (Reed, 1961).

Volcanic Rocks of Foraker Glacier

The late Paleocene and early Eocene volcanic rocks outcrop along the north flank of the Alaska Range in the vicinity of the McKinley Fault Zone (fig. 2). We studied these rocks along the west side of the Foraker Glacier (fig. 4), where the volcanic sequence is more than 2,000 m thick and unconformably overlies 610 m of sedimentary rocks (fig. 5). The sedimentary sequence beneath the volcanic rocks is significant because it records an episode of tectonic uplift and basin subsidence before volcanism.

Late Cretaceous(?) Sedimentary Rocks

Lithology and Stratigraphy

The base of the sedimentary sequence is a well-exposed angular unconformity above folded schist and metasedimentary rocks (fig. 6). The contact can be traced for several kilometers along strike (fig. 4). The stratigraphically lowest sedimentary unit is a 230-m-thick boulder to cobble conglomerate. This unit is coarsest in the lower 100 m, where clasts typically range from 0.4 to 1.2 m in diameter, with maximum clast sizes of more than 2 m in diameter. This unit fines upward and is a cobble-pebble conglomerate in the uppermost 20 to 30 m. Matrix consists of medium grained to pebbly sandstone. The conglomerate is poorly to moderately sorted, mostly clast supported, and occurs in poorly defined 1- to 5-m-thick beds. The bases of beds are typically scoured with a few to tens of centimeters of relief. Conglomerate beds range in texture from poorly organized and massive with randomly arranged clasts to well organized with imbricated clasts, planar crossbedding, and normal grading. The poorly organized conglomerate is more abundant than the well-organized conglomerate. Interbedded throughout the conglomerate are 15- to 60-cm-thick, trough-cross-stratified, medium- to coarse-grained sandstone beds that are lenticular and typically reach a few meters in width. Also interbedded with the conglomerate are 30- to 60-cm-thick, dark-gray, pebbly mudstone beds. These beds are matrix supported, poorly sorted, and drape underlying conglomerate beds.

Clast composition of the lower conglomerate unit is almost entirely metamorphic (fig. 5). The metamorphic-rock clasts include muscovite-quartz schist, quartzite, and argillite, which are the same rock types as the metamorphic rocks that underlie the conglomerate. Paleoflow data, on the basis of conglomerate-clast imbrication, show a westward and southwestward drainage pattern (fig. 7).

Overlying the lower conglomerate unit are alternating intervals (ranging from about 65 to 115 m in thickness) of dark-gray mudstone, sandstone, and conglomerate (fig. 5). The

mudstone intervals are mostly dark-gray shale with very thin to thin interbeds of siltstone. The siltstone displays horizontal, low-angle, and ripple cross-stratification. Some shale intervals contain abundant plant fragments. The sandstone-conglomerate intervals include medium- to coarse-grained gray to tan ("salt and pepper") lithic sandstone and pebble to cobble conglomerate with thin interbeds of dark-gray shale. The sandstone beds typically range from 0.3 to 1 m in thickness, and the conglomerate beds average 0.5 to 2 m in thickness. The sandstone beds commonly display trough cross-stratification and range in texture from massive to horizontally laminated. Pebbly sandstone lenses are common within the axial parts of large-scale troughs. The conglomerate beds are lenticular, well sorted, and clast supported and in some areas display well-developed clast imbrication. Average clasts range from 1 to 5 cm in diameter. The conglomerate beds typically have erosional bases and commonly grade upward into trough-cross-stratified sandstone beds. Clasts in the upper conglomerate unit are primarily argillite, quartzite, and chert, with minor amounts of sandstone and schist.

The sedimentary rocks unconformably overlie folded Paleozoic metamorphic rocks of uncertain, possibly Devonian and Carboniferous age (Reed, 1961) and are overlain unconformably by the volcanic rocks of Foraker Glacier (fig. 4). Samples of mudstone from the middle and upper parts of the sedimentary sequence were analyzed for pollen but were found to be barren (S. Reid, written commun., 1999). Although a precise age control for these strata does not yet exist, a working hypothesis is that they are equivalent to the Late Cretaceous lower Cantwell Formation described and dated in the Healy quadrangle by Ridgway and others (1997). The strata beneath the volcanic rocks of Foraker Glacier are bounded below and above by unconformities, as is the lower part of the Cantwell Formation in the Healy quadrangle (Ridgway and others, 1997; Cole and others, 1999). Also, the sedimentary strata near Foraker Glacier and the lower Cantwell strata in the Healy quadrangle are overlain by coeval volcanic

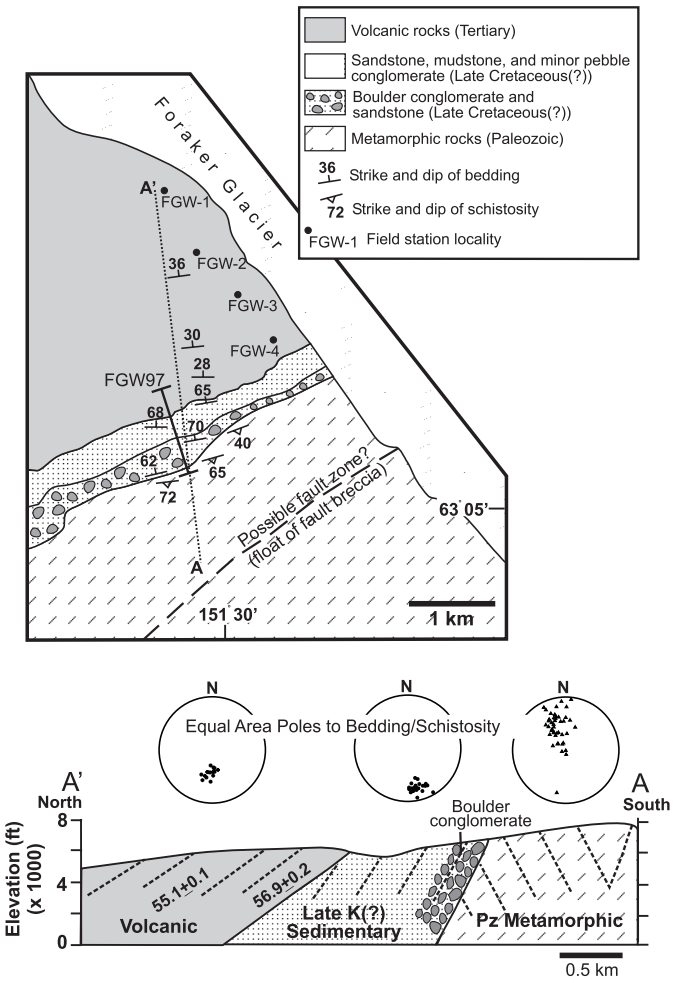

Figure 4. Generalized geologic map and cross section for units exposed in the Foraker Glacier area, south-central Alaska (fig. 2). FGW97, location of the composite stratigraphic column shown in figure 5. Stereonets are lower-hemisphere equal-area projections of poles to bedding for sedimentary- and volcanic-rock units and poles to youngest observable schistosity in metamorphic rocks.

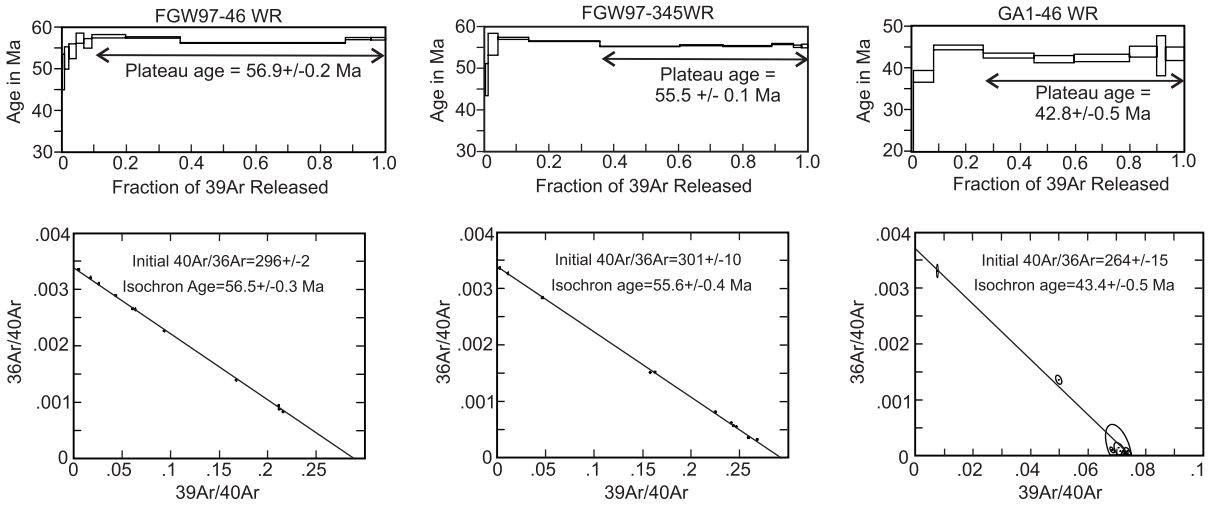

Figure 3. $^{40}Ar/^{39}Ar$-plateau ages and isochron plots for samples from the volcanic rocks of Foraker Glacier and the Mount Galen Volcanics. See figure 2 for locations and figures 8 and 12 for stratigraphic positions of samples.

Table 1. Compilation of radiometric ages for volcanic rocks in the Mount McKinley quadrangle.

Sample	Unit/location	Description	Material dated[1]	Age (Ma)[2]	Notes[3,4]
This study ($^{40}Ar/^{39}Ar$ step heating)[3]					
GA1–46	Mount Galen Volcanics. North side of Mount Galen in the Mount McKinley B–1 1:63,360-scale quadrangle, lat 63°28′19″ N., long 150°21′22″ W.	Basalt, 46 m above the base of the Mount Galen Volcanics.	W W	**42.8±0.5** 43.4±0.5	Plateau age. Isochron age.
FGW–46	Volcanic rocks of Foraker. Glacier/west side of Foraker Glacier in the Mount McKinley A–3 1:63,360-scale quadrangle, lat 63°05′45″ N., long 151°24′49″ W.	Basalt; 46 m above the base of the volcanic rocks of Foraker Glacier.	W W	**56.9±0.2** 56.5±0.3	Plateau age. Isochron age.
FGW–345	Volcanic rocks of Foraker. Glacier/west side of Foraker Glacier in the Mount McKinley A–3 1:63,360-scale quadrangle, lat 63°5′52″, long 151°24′53″ W.	Porphyritic rhyolite; 345 m above the base of the volcanic rocks of Foraker Glacier.	W W K K	55.5±0.1 55.6±0.4 **54.6±0.2** 55.4±0.3	Plateau age. Isochron age. Plateau age. Isochron age.
Previous K-Ar studies[5]					
1	Mount Galen volcanics----------	Andesite----------	P H	41.1±1.2 38.9±1.1	$^{40}Ar_{rad}/^{40}Ar_{total}$=0.652 $^{40}Ar_{rad}/^{40}Ar_{total}$=0.554
2	Mount Galen volcanics----------	Basalt----------	P	34.8±1.4 35.7±1.4 (minimum ages)	$^{40}Ar_{rad}/^{40}Ar_{total}$=0.734 $^{40}Ar_{rad}/^{40}Ar_{total}$=0.743
3	Mount Galen volcanics----------	Basalt----------	P	39.6±1.2 (minimum age)	$^{40}Ar_{rad}/^{40}Ar_{total}$=0.481
6	Mount Galen volcanics----------	Andesite----------	H	38.7±1.1	$^{40}Ar_{rad}/^{40}Ar_{total}$=0.435
4	West side of Muldrow Glacier -----	Basalt----------	P	33.1±1.0 (minimum age)	$^{40}Ar_{rad}/^{40}Ar_{total}$=0.586

[1]Materials: H, hornblende; K, K-feldspar; P, plagioclase; W, whole rock.
[2]Preferred ages shown in bold.
[3]Laser: Step-heated using an Ar-ion laser, measured on a VG3600 spectrometer. Furnace: Step-heated using a resistance-type furnace, measured on a Nuclide 6–60–SGA spectrometer.
[4]Ages of this study were run against standard Mmhb–1 with an age of 513.9 Ma and processed by using standards of Steiger and Jäger (1977). Error limits, ±1σ. Analytical data and age spectra are available from the authors on request.
[5]Age data reported by Decker and Gilbert (1978) corrected according to Dalrymple (1979); sample numbers refer to map numbers of Decker and Gilbert (1978).

rocks. Finally, the sedimentary strata along Foraker Glacier contain lithofacies that are similar to the lower part of the Cantwell Formation in the Healy quadrangle.

Interpretation

We interpret these sedimentary strata to record a significant episode of tectonic uplift and basin subsidence before the onset of late Paleocene and early Eocene volcanism in the region. The very large clast size of the lower conglomerate unit indicates proximity to an uplifted source area, and the clast compositions, along with the basal angular unconformity, indicate that the underlying metamorphic rocks were part of this uplift. Collectively, the rocks in the lower conglomerate unit are typical of alluvial-fan deposits. We interpret the poorly organized conglomerate facies as the deposits of high-concentration stream floodflows and (or) noncohesive debris flows.

The absence of internal stratification and the poor sorting of these deposits preclude dilute streamflow bedload deposition. Also, the absence of muddy matrix and the clast-supported fabric indicates deposition from high-concentration water-sediment dispersions or fines-depleted debris flows (Costa, 1988). Similar types of deposits were described by Allen (1981), Nemec and Steel (1984), and DeCelles and others (1991) as thick sheets on alluvial-fan surfaces. The massive pebbly sandstone and the trough-crossbedded sandstone interbeds were most likely deposited during waning flood stages by hyperconcentrated flows and more dilute-phase streamflows (Pierson and Scott, 1985; Smith, 1986). The well-organized and imbricated conglomerate facies and trough-cross-stratified sandstone interbeds represent episodes of dilute-phase floodflows and streamflows, respectively (Costa, 1988).

The thick intervals of mudstone and sandstone-conglomerate that overlie the lower conglomerate unit probably represent a period of basin subsidence with intermittent episodes of renewed tectonic uplift and (or) shifting drainage systems. During this period, ponded environments (lakes, swamps) formed in the basin, and the mudstone intervals were deposited. The sandstone-conglomerate intervals represent the influx of braided fluvial systems into the ponded environments. This fluvial influx could represent progradation during periods of tectonic uplift, or simply changes in drainage patterns or source-rock types within the basin (for example, DeCelles and others, 1991).

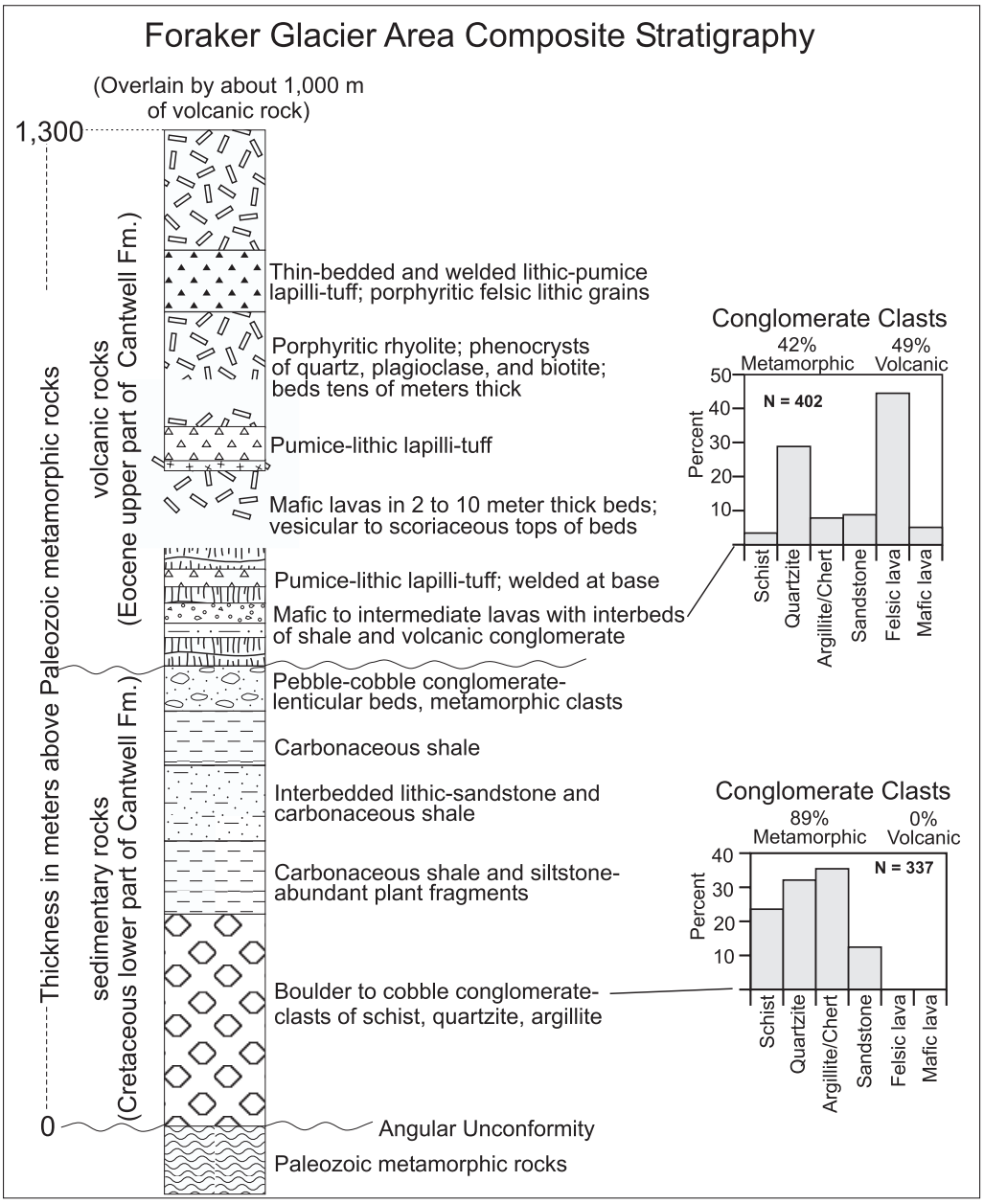

Figure 5. Composite stratigraphic column for the Foraker Glacier area, south-central Alaska (fig. 2). Histograms show conglomerate-clast-count data.

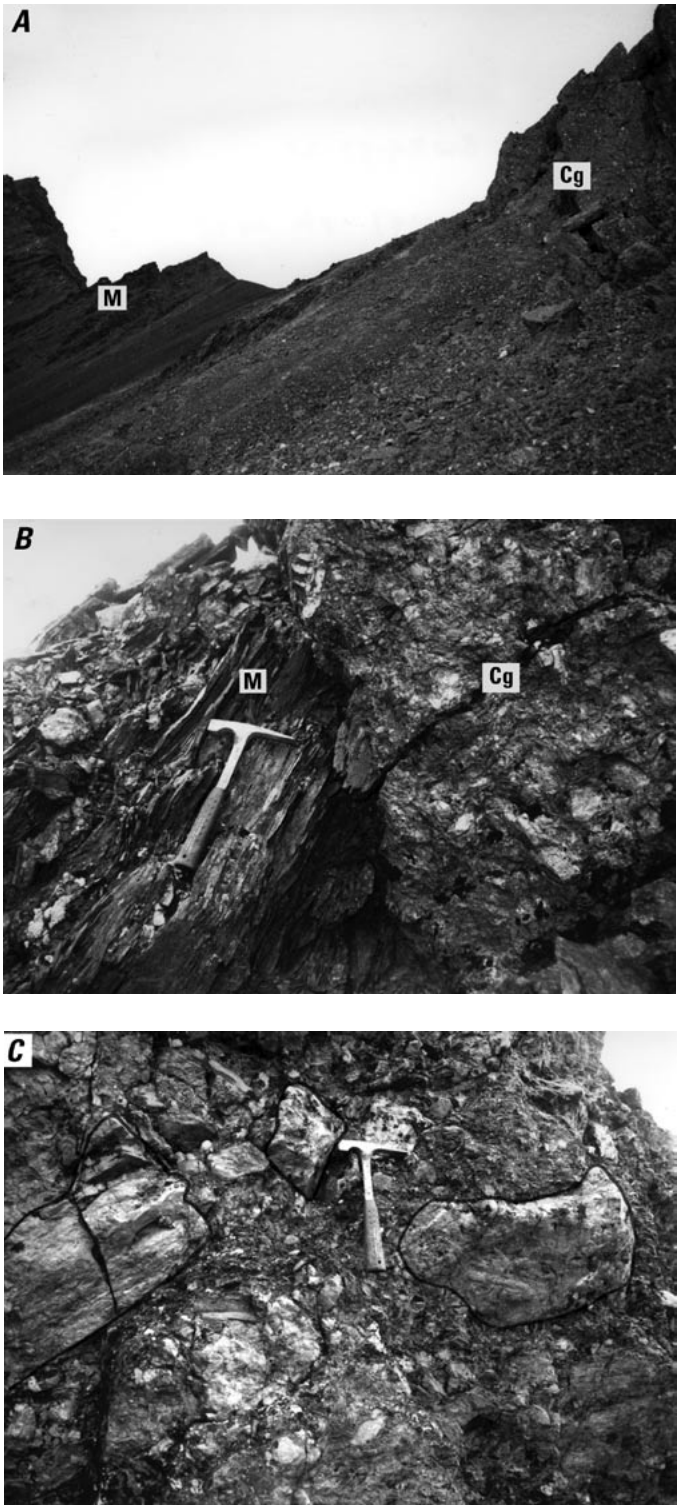

Figure 6. Paleozoic-Late Cretaceous(?) contact along west side of Foraker Glacier (fig. 2). *A* and *B*, Nonconformable contact between south-dipping Paleozoic metamorphic rocks (M) and north-dipping Late Cretaceous(?) cobble to boulder conglomerate (Cg). *C*, Cobble to boulder conglomerate about 5 m above Paleozoic contact. Boulder-size metamorphic clasts are outlined.

Volcanic Rocks

Lower Basalt-Andesite and Sedimentary Sequence

The late Paleocene and early Eocene volcanic rocks are unconformable with the underlying sedimentary sequence and generally dip about 35º–45º N. (fig. 4). The lowermost part of the volcanic sequence includes basalt and andesite lavas that are interbedded with sedimentary rocks (figs. 8, 9). The andesite lavas and sedimentary rocks are present only in the lowest 100 m of this sequence. The basalt lavas are brown to dark gray in flows that range from 2 to 18 m in thickness (avg 5–6 m thick). Many flows are columnar jointed and have vesicular tops; some basalt flows have thin to thick scoriaceous upper zones that weather yellow-red. In thin section, the basalt contains euhedral to subhedral plagioclase laths (An_{40} to An_{70}) with minor amounts of continuous zoning. Clinopyroxenes and olivine are present but are very fine grained and occupy interstices in the groundmass between the plagioclase laths. Needles and equant grains of opaque minerals (Fe-Ti oxides) are also present. There is some calcite replacement of plagioclase and some alteration of groundmass into clay minerals. The andesite lavas are less abundant than the basalt, occur in flows that range from 2 to 12 m in thickness, have tabular to lenticular bed shapes, are medium gray to brown, have few vesicles, and are typically porphyritic. The andesite consists almost entirely of plagioclase (An_{50} to An_{88}) with needles and equant grains of Fe-Ti oxides and trace amounts of biotite. Plagioclase is euhedral to subhedral and commonly displays resorption textures and reaction rims. Continuous zoning is common. The

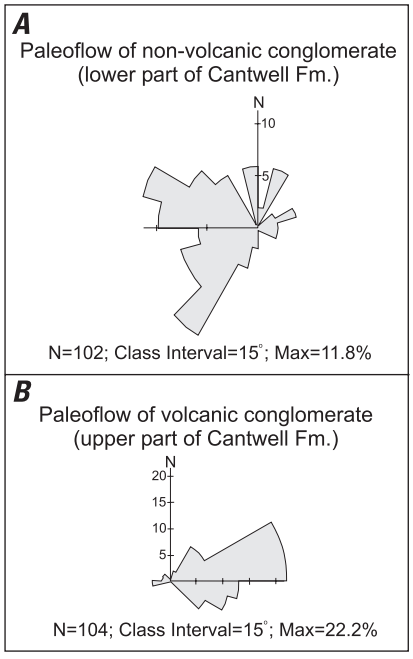

Figure 7. Paleocurrent rose diagrams for fluvial conglomerates along west side of Foraker Glacier (fig. 2), as measured from imbricated clasts and restored by using average bedding for each unit. *A*, Westward-directed paleoflow for cobble-boulder conglomerate within 100 m above Paleozoic metamorphic rocks. *B*, Eastward-directed paleoflow for two intervals of pebble-cobble conglomerate within lowermost 72 m of volcanic-rock unit.

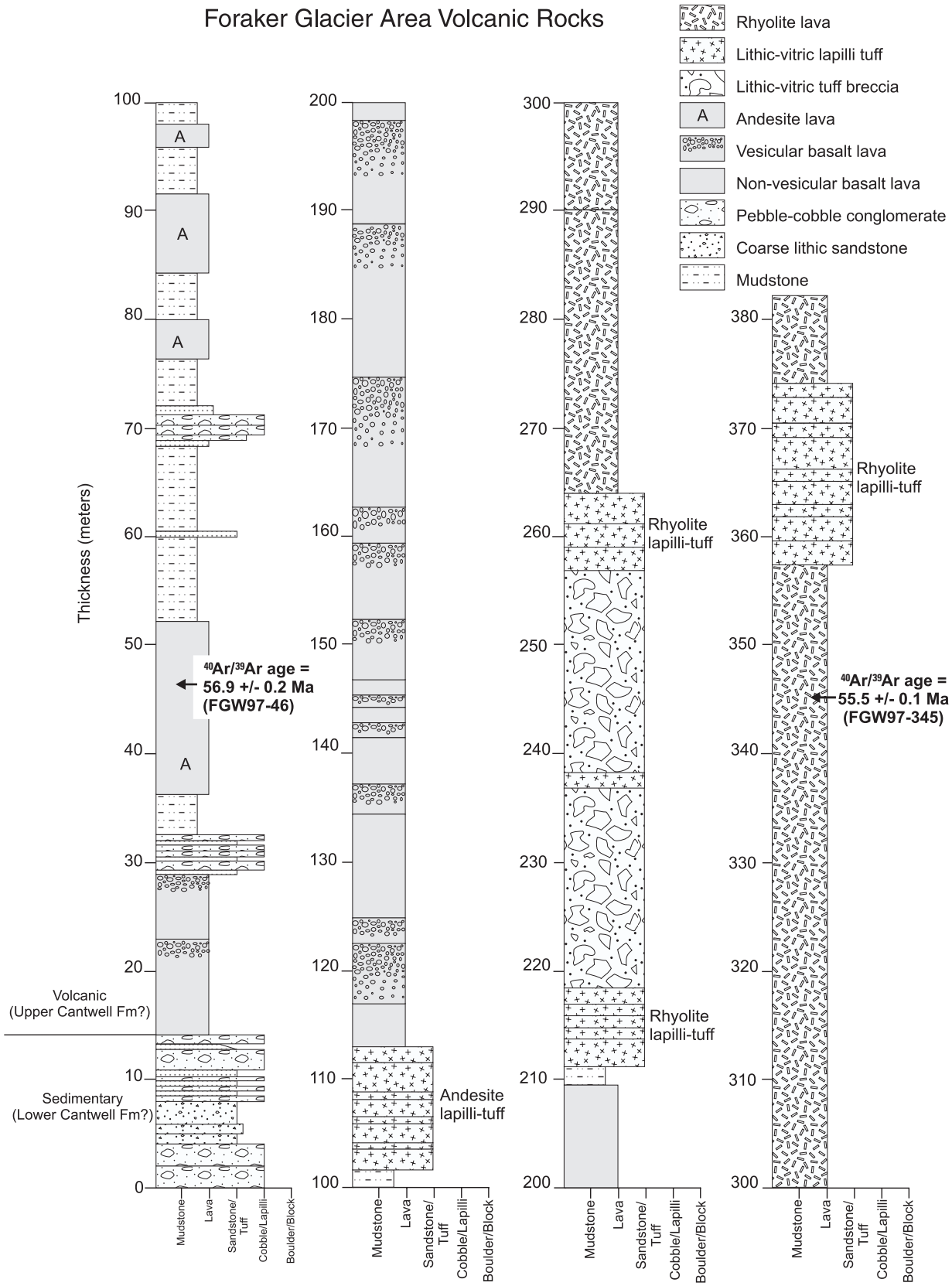

Figure 8. Detailed stratigraphic column for lowermost volcanic rocks of Foraker Glacier (fig. 2), measured bed by bed by using a Jacob staff. Note stratigraphic positions of two new $^{40}Ar/^{39}Ar$ radiometric ages reported in this study.

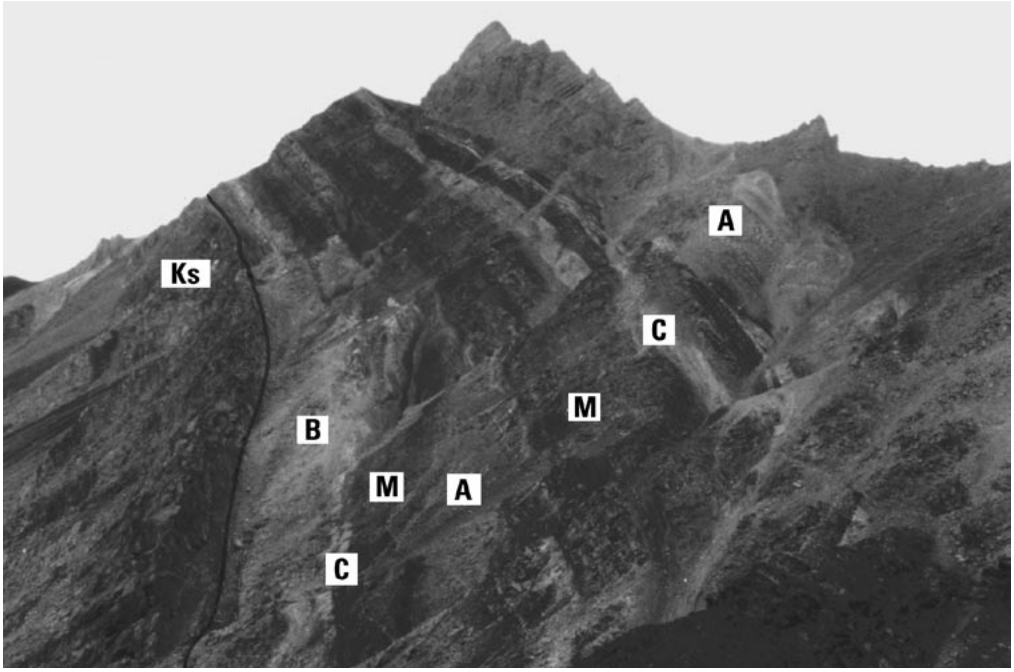

Figure 9. Lowermost interval of volcanic and sedimentary rocks exposed along west side of Foraker Glacier (fig. 2). Volcanic rocks sharply overlie interval of pebble-cobble conglomerate at top of Late Cretaceous(?) sedimentary rocks (Ks); contact is at about 14-m level in stratigraphic column (fig. 8). Tertiary volcanic and sedimentary units: A, andesite lava; B, basalt lava; C, conglomerate; M, mudstone with interbedded fine-grained sandstone.

groundmass consists of microcrystalline plagioclase, devitrified glass, and opaque minerals.

The sedimentary rocks interbedded with the basalt and andesite lavas include shale-siltstone and conglomerate intervals. The shale-siltstone intervals range from 3 to 9 m in thickness and include fissile dark-gray to black shale, with 0.5- to 5-cm-thick dark-gray siltstone to very fine sandstone beds. The siltstone and very fine sandstone beds display horizontal, low-angle, and climbing ripple laminations, and some beds contain groove and flute casts at their bases. All of these intervals contain abundant plant fragments and very thin (a few millimeters thick) coal seams. Two conglomerate intervals that are each about 6 m thick (fig. 8) consist of 0.3- to 0.8-m-thick beds of clast-supported, moderately sorted to well-sorted pebble-cobble conglomerate (clast size, avg 3–5 cm, max 9–10 cm in diameter). The conglomerate ranges in texture from massive to imbricated and contains 0.2- to 0.5-m-thick interbeds of lenticular, trough-crossbedded coarse sandstone. The conglomerate contains 49 percent volcanic clasts (mostly medium-gray porphyritic felsic rhyolite-dacite), 42 percent metamorphic clasts (mostly quartzite), and 9 percent sandstone clasts (fig. 5). Paleoflow as measured from clast imbrication in the conglomerate intervals was eastward (fig. 7).

Rhyolite Lavas and Pyroclastic Deposits

Rhyolite lavas and pyroclastic deposits are the most abundant volcanic rocks in the Foraker Glacier area. At least 1,500 m of felsic volcanic rocks overlies the lower interval of intermediate and mafic lavas (figs. 4, 5). The rhyolite lavas are medium to light gray and porphyritic, weather light gray and light purple, and occur as massive intervals with poorly defined bed contacts. Some intervals are flow banded and display red-gray wispy layering. The more massive intervals are columnar jointed. In thin section, the rocks show a groundmass of devitrified glass with spherulitic texture and microlites of feldspar and quartz. The phenocrysts include quartz, alkali feldspar, and biotite. The quartz is euhedral to subhedral, showing bipyramidal forms, and is commonly embayed. The alkali feldspar is mostly orthoclase (2V angle, >60º) in subhedral rectangular to equant grains. Graphic intergrowth with quartz and exsolution textures are common. The biotite is strongly oxidized and is present as only a small percentage of the modal mineralogy.

Two pyroclastic lithofacies occur within the volcanic sequence along Foraker Glacier. The first lithofacies is a thin-bedded lithic-crystal lapilli tuff, and the second is a massive lithic tuff-breccia. The lapilli tuff is light to medium gray and occurs in 3- to 8-m-thick intervals that consist of 1- to 8-cm-thick horizontally laminated beds. Individual laminations within beds range from a few millimeters to 20 mm in thickness and consist of alternating fine and coarse couplets with finer grained crystal-lithic-rich bases and pumice-rich tops. Grain size in the first lithofacies is predominantly 1 to 5 mm, with scattered thin and discontinuous lenses of lithic grains, as much as 2 to 3 cm in diameter. Parts of this lithofacies are welded and exhibit a strong eutaxitic texture defined by flattened and aligned pumice and glass shards. Two compositional types of the first lithofacies, andesitic and rhyolitic, can be defined on the basis of crystal composition. The andesitic lapilli tuff occurs in only one stratigraphic interval at the top of the basalt-andesite sedimentary sequence, 102 to 115 m above the base of the volcanic rocks (fig. 8). This first compositional type

is characterized by crystals of quartz, plagioclase, and minor biotite and by pumice grains with large, thick-walled vesicles. The rhyolitic lapilli tuff is interbedded with the rhyolite lavas and includes crystals of quartz, alkali feldspar with exsolution and graphic textures, and rare plagioclase, with finely vesicular and wispy pumice grains. Both compositional types contain cuspate and bladed vitric shards (mostly devitrified) and include similar accidental lithic grain populations of basalt, schist, sandstone, and polycrystalline quartz. The second compositional type also contains lithic grains of porphyritic rhyolite (similar in texture and mineralogy to the rhyolite lavas).

The second lithofacies is white to light gray and occurs in 14- to 20-m-thick intervals with poorly defined bedding contacts. This lithofacies, which typically overlies the first lithofacies (fig. 8), is massive and poorly sorted and exhibits inverse grading at the base of each interval. Quartz is the predominant crystal in the second lithofacies and is present as euhedral, subhedral, and broken or shattered grains. The groundmass consists of devitrified fine ash and relict cuspate shards. Lapilli to block-size lithic clasts (2–30 cm in diameter) are mostly laminated to welded rhyolitic lapilli tuff and porphyritic rhyolite (glassy groundmass with phenocrysts of quartz and alkali feldspar). A trace (<2 volume percent) of nonvolcanic grains (sandstone and polycrystalline quartz) is present.

Interpretation

The late Paleocene and early Eocene volcanic episode in the Foraker Glacier area began with the outpouring of basalt and andesite lavas. These lavas flowed into a tectonically active basin, the fill of which is represented by the underlying sedimentary deposits. The presence of an angular unconformity at the base of the volcanic rocks implies that the area underwent an episode of uplift before volcanism; this uplift could have been partly caused by thermal doming associated with the onset of volcanism or might represent an episode of tectonic shortening that preceded volcanism. The absence of pyroclastic deposits in the lowermost part of the volcanic sequence suggests that the lavas were erupted from fissures within or close to the basin. We interpret the mudstone and siltstone deposits that are interbedded with the basalt and andesite lavas to represent background sedimentation within the basin between eruptions. The conglomerate intervals interbedded with the lowermost lavas contain an abundance of porphyritic rhyolite clasts; we interpret these conglomerates to represent synvolcanic sedimentation during the onset of felsic volcanism at a more distant ventsite. The lenticular shape of beds, well-developed imbrication of rounded clasts, clast-supported framework, and trough-crossbedded sandstone all indicate deposition from braided fluvial systems (Rust, 1972; Miall, 1977; Costa, 1988). These streams flowed eastward through the basin, possibly draining volcanic source areas to the west and southwest. The mixture of volcanic and metamorphic clasts implies that even during the onset of felsic volcanism there was continued erosion of metamorphic source rocks and (or) erosion of the Late Cretaceous(?) metamorphic-clast conglomerate.

The presence of the andesitic lapilli tuff interval interbedded with the basalt lavas is the first sign of explosive volcanism recorded in the basin. Explosive volcanism became most pronounced after the effusion of the basalt lavas when about 50 m of rhyolitic thin-bedded lapilli tuff and tuff breccia was deposited. The composition of the lapilli tuff and tuff breccia (vitric shards, pumice, euhedral to subhedral crystals, volcanic lithic grains, and only traces of nonvolcanic lithic grains), along with the presence of welding, indicates that these are primary pyroclastic deposits. We interpret these facies as pyroclastic-surge and pyroclastic-flow deposits, respectively. Pyroclastic surges are dilute, turbulent flows of hot gas and ash that form during explosive eruptions and can be independent or cogenetic with denser, high-concentration pyroclastic flows (Fisher, 1979; Wright and others,1980). The andesitic lapilli tuff and the lowermost rhyolitic lapilli tuff (fig. 8) most likely represent pyroclastic-surge deposits that formed during relatively smaller pulses of explosive eruptions, possibly signaling the early growth of the felsic eruptive center. Intervals of pyroclastic-surge deposits have also been documented to mark the beginning of felsic eruptive episodes in other volcanic settings (for example, Cole and DeCelles, 1991). The laminations and alternating fine-coarse couplets of this facies most likely represent traction-carpet sedimentation along the base of flows, similar to that of high-density turbidity flows (Lowe, 1982). Pyroclastic-flow deposits are commonly described in terms of flow units, which are produced during the passage of a single pyroclastic flow. Pyroclastic-flow units typically are inversely graded, with crudely laminated lower intervals (commonly tens of centimeters thick) and massive, poorly sorted upper zones (Sparks and others, 1973; Fisher, 1979). The second lithofacies includes at least two major pyroclastic-flow units but may consist of several amalgamated pyroclastic-flow deposits with poorly defined contacts. This episode of pyroclastic-flow deposition marks a more explosive interval during the early phase of felsic volcanism. After this phase, the basin was inundated by rhyolite lavas and additional pyroclastic deposits. The ventsites for this phase of volcanism were most likely within a few kilometers of the basin because rhyolite lavas are highly viscous and typically flow no more than a few kilometers from their vents (Cas and Wright, 1987).

Mount Galen Volcanics

The Mount Galen Volcanics, of late Eocene and early Oligocene age, is exposed on the west side of the Muldrow Glacier terminus and in the Mount Galen area (fig. 2). The base of the volcanic sequence in the Muldrow Glacier area is not exposed, but in the Mount Galen area the volcanic rocks unconformably overlie interbedded sandstone and shale of the lower part of the Cantwell Formation. The rocks in these two areas are described separately below.

Muldrow Glacier Area

Approximately 280 m of volcanic rocks is exposed along the west side of the Muldrow Glacier terminus (figs. 10, 11). This exposure consists mostly of pyroclastic deposits with

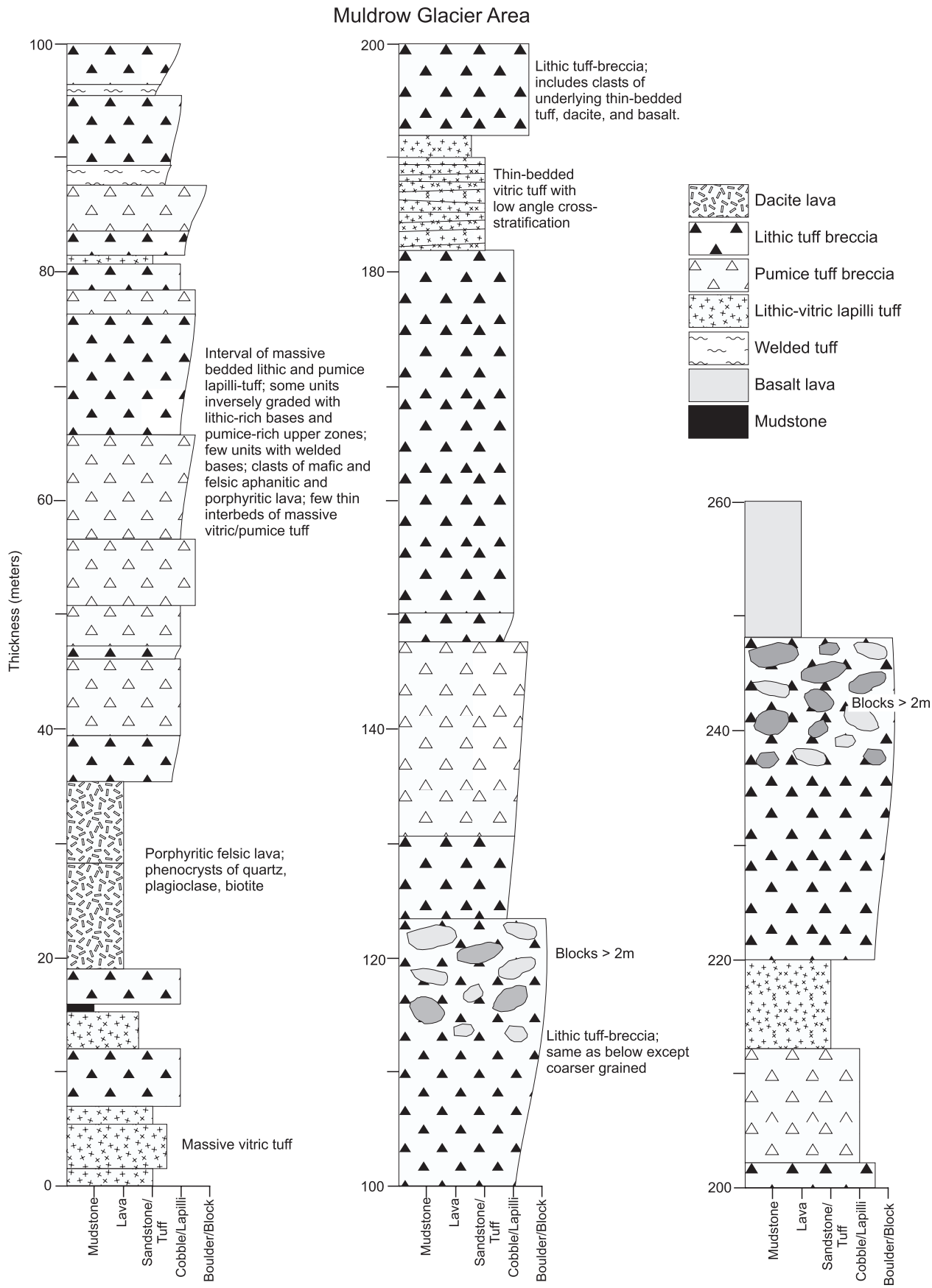

Figure 10. Stratigraphic column for the Mount Galen Volcanics exposed along west side of Muldrow Glacier terminus (fig. 2), measured bed by bed by using a Jacob staff. Light-shaded blocks, basalt; dark-shaded blocks, felsic lava.

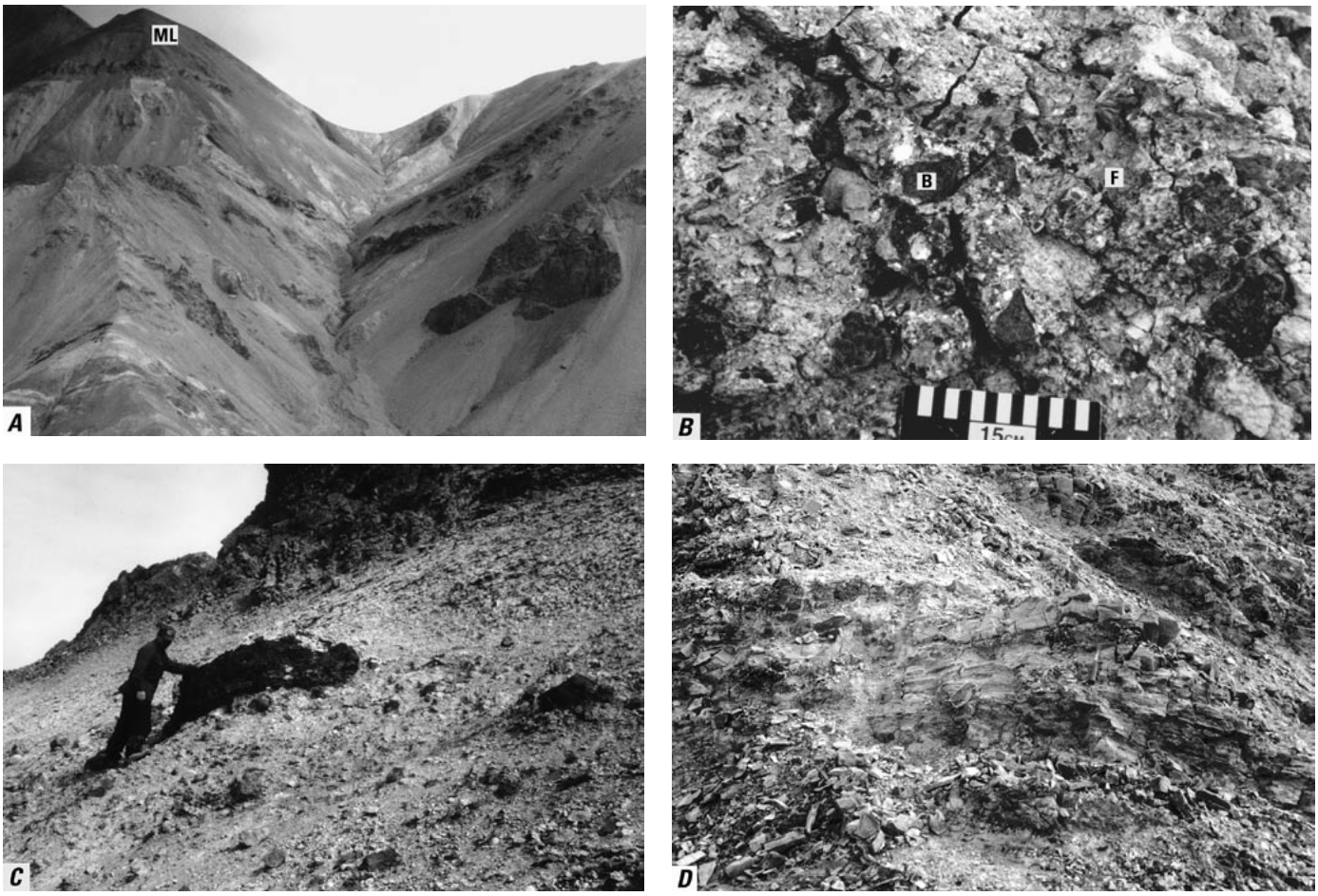

Figure 11. Characteristics of pyroclastic rocks in the Mount Galen Volcanics in Muldrow Glacier area (fig. 2). *A*, Exposed section of volcanic rocks, showing pyroclastic deposits capped by mafic lava (ML); view westward. *B*, Lithic-lapilli-tuff facies with clasts of porphyritic felsic lava (F) and basalt (B). *C*, Large block of basalt within lithic-tuff-breccia facies. *D*, Thin-bedded vitric-tuff facies.

intervals of felsic lavas (dacite and minor rhyolite) and basaltic lavas. All of these volcanic deposits show some degree of alteration; many of the pyroclastic deposits, especially finer grained tuff beds, are strongly altered to clay minerals and chlorite. Secondary pyrite is common in tuff deposits within the lower 50 m of the exposed volcanic sequence.

The felsic lavas, which occur in the stratigraphically lowest part of the exposure, are porphyritic, with phenocrysts of plagioclase, alkali feldspar, and quartz. The plagioclase is commonly euhedral, discontinuously zoned, and Na rich (An_{20} to An_{50}). The alkali feldspar is subhedral, with partial alteration to clay minerals, and displays graphic intergrowths with quartz. The groundmass ranges in texture from a devitrified glass to a microlitic trachyte. The basaltic lavas (basalt to basaltic andesite) occur near the top of the exposed volcanic sequence (figs. 10, 11*A*). The rocks are aphanitic to porphyritic and consist mostly of plagioclase, with smaller amounts of altered pyroxene, opaque minerals, and devitrified glass in the spaces between plagioclase laths.

The pyroclastic deposits are primarily massive intervals of light-gray to light-purple lithic tuff-breccia and pumice lapilli tuff, with minor amounts of interbedded vitric tuff (fig. 10). The lithic tuff-breccia forms massive deposits that range from 1 to 32 m in thickness. The thicker intervals probably include amalgamated beds, but except for the bases and tops of each interval, bedding contacts within these deposits are poorly defined. Inverse grading is common at the bases of these deposits, and the upper parts typically are more pumiceous. The deposits are poorly sorted and contain angular to subrounded clasts (fig. 11*B*). The lithic clasts in these deposits typically range from 0.5 to 5 cm in diameter, but the two thickest deposits contain blocks as much as 2 m across (fig. 11*C*). Lithic-clast types include light-gray to light-purple porphyritic rhyolite (similar to the rhyolite in the lower part of the volcanic sequence), brown to dark-gray mafic aphanitic lava (basalt and basaltic andesite with intersertal and trachytic texture), light-gray pumice tuff, granite, and minor sandstone. Groundmass material is mostly devitrified glass containing wispy pumice grains, relict cuspate vitric shards, and crystals of plagioclase, quartz, and biotite.

The pumice-rich lapilli tuff occurs in 2- to 17-m-thick, poorly sorted intervals, some of which display inverse grading. These intervals are characterized by abundant pumice, which ranges in clast size from 0.5 to 10 cm across. Groundmass in the deposits consists of devitrified cuspate shards, wispy pumice, euhedral to subhedral plagioclase, and subhedral

quartz. A small percentage of lithic grains in these deposits includes mostly aphanitic and porphyritic rhyolite and vitric tuff. Many intervals of the pumice-rich lapilli tuff are gradational with underlying lithic tuff-breccia deposits.

The vitric-tuff deposits are light to dark gray, yellow, and green and range from about 1 m to 8 m in thickness. These deposits form massive to thin-bedded intervals with horizontal and low-angle stratification (fig. 11*D*). The tuff deposits contain mostly devitrified cuspate shards and wispy pumice grains, with scattered quartz and plagioclase crystals.

The volcanic sequence near Muldrow Glacier records an episode of pyroclastic eruptions with intermittent lava flows. The lithic-tuff-breccia intervals that grade upward into pumice-rich lapilli tuff are typical of pyroclastic-flow deposits, in which the denser lithic clasts are commonly concentrated near the bases of flows, while pumice is rafted along the tops of flows (Walker, 1971; Sparks, 1976). The massive and thin-bedded vitric tuff probably formed as pyroclastic-fallout and pyroclastic-surge deposits, respectively. The horizontal and low-angle stratification in the thin-bedded tuff is characteristic of low-density pyroclastic-surge deposits (Fisher, 1979). Pyroclastic-fallout deposits are typically massive, with even bed contacts (Fisher and Schmincke, 1984), similar to the characteristics observed for the massive vitric tuff facies.

Mount Galen Area

The Mount Galen Volcanics was first named and described by Decker and Gilbert (1978), who defined the type locality at Mount Galen in the northwest corner of the Mount McKinley B–1 1:63,360-scale quadrangle. The unit has a minimum thickness of 1,000 m and consists of basalt and andesite lavas and andesite to dacite pyroclastic deposits (Decker and Gilbert, 1978). We report a new reference stratigraphic section through the lower 250 m of the Mount Galen Volcanics (fig. 12), along with new geochemical data for these rocks (described below). The basalt lavas occur in beds a few meters to 30 m thick and are commonly columnar jointed. Many of the basalt and andesite lava flows exhibit brecciated and vesicular upper zones. In some places, the lavas appear as volcanic breccia and are most likely lava autobreccia deposits because the groundmass is identical to the clasts and vesicles crosscut clast and matrix boundaries. Decker and Gilbert described the basalts as holocrystalline and porphyritic, with phenocrysts of clinopyroxene, zoned plagioclase (An_{55} to An_{60}), magnetite, and olivine (listed in order of decreasing abundance). The basalt groundmass is mostly plagioclase microlites containing scattered Fe-Ti oxides and small amounts of devitrified glass. There are two varieties of andesite in the Mount Galen Volcanics: a hornblende andesite and a less abundant two-pyroxene andesite (Decker and Gilbert, 1978). The hornblende andesite is porphyritic, with a glassy to microcrystalline groundmass. The most abundant phenocryst is plagioclase (An_{52} to An_{65}), which occurs as euhedral to subhedral rectangular to blocky grains and commonly exhibits continuous zoning and resorption textures. Hornblende is commonly zoned and also shows resorption textures. The two-pyroxene andesite is porphyritic and includes euhedral to subhedral plagioclase, with oscillatory zoning and resorption textures, euhedral to subhedral and zoned hypersthene, euhedral to subhedral and twinned augite, and Fe-Ti oxides within a groundmass of microlitic plagioclase (Decker and Gilbert, 1978).

Pyroclastic deposits in volcanic rocks of the Mount Galen area include vitric-lithic tuff to lapilli tuff and lithic tuff-breccia. These deposits are most conspicuous in a thick interval above the lowermost lavas (fig. 12). A thick, massive vitric tuff also marks the base of the Mount Galen Volcanics in this area. The vitric-lithic lapilli tuff and tuff-breccia are similar in composition and vary mostly in grain size. The lapilli tuff contains lithic and pumice grains that are generally 1 to 4 cm across, and the tuff-breccia contains angular to subrounded lithic blocks as large as 1 to 5 m in diameter (fig. 13). The lapilli tuff occurs in thinner (1–4 m thick) intervals that display faint horizontal to low-angle stratification. The tuff breccia occurs in very thick (5–60 m thick) intervals that are massive and commonly are inversely graded in their lower third. Common lithic clasts in these deposits include hornblende and two-pyroxene andesite, basalt, vitric tuff, and felsic porphyritic lava (phenocrysts of plagioclase, biotite, and quartz in a microlitic and devitrified groundmass).

The Mount Galen Volcanics records an initial pyroclastic eruption (tuff layer at base) followed by effusion of basalt and andesite lavas. The lava eruptions were followed by an interval of explosive volcanism. The lithic lapilli tuff and tuff-breccia facies consist almost entirely of juvenile volcanic grains (vitric shards, euhedral-subhedral crystals, porphyritic lava) and are primary pyroclastic deposits. The thin-bedded and laminated lapilli-tuff facies most likely represents deposition from pyroclastic surges, and the tuff-breccia facies consists of deposits derived from dense pyroclastic flows generated by more explosive eruptions. (See sections above for discussions of these types of pyroclastic deposits.)

Volcanic-Rock Geochemistry

We report new major- and trace-element data on 14 samples from the volcanic rocks of Foraker Glacier and 17 samples from the Mount Galen Volcanics (9 from the Muldrow Glacier area and 8 from the Mount Galen area; tables 2, 3). These data are the first published geochemical analyses for volcanic rocks of the Foraker Glacier and Muldrow Glacier areas, and the first set of trace-element analyses for the Mount Galen Volcanics. Decker and Gilbert (1978) reported major-element data for six samples of the Mount Galen Volcanics.

Although all of these volcanic rocks are subalkalic, the volcanic rocks of Foraker Glacier and the Mount Galen Volcanics differ in major- and trace-element chemistry. On the basis of major-element chemistry, the volcanic rocks of Foraker Glacier are a basalt-andesite-rhyolite suite, whereas the Mount Galen Volcanics is primarily a basaltic andesite-andesite-dacite suite, although minor basalt and rhyolite is present (fig. 14). In addition, the volcanic

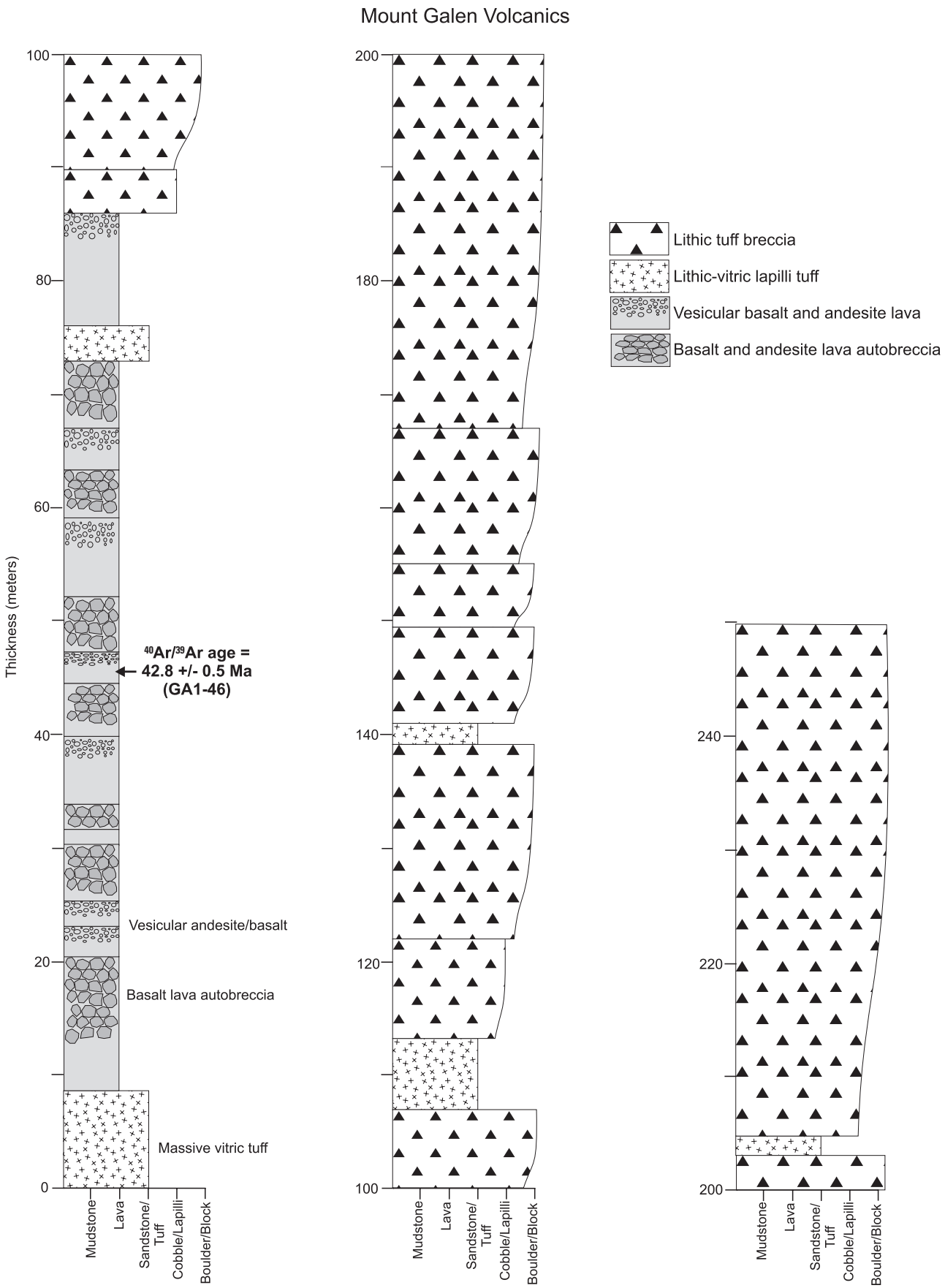

Figure 12. Stratigraphic column for the Mount Galen Volcanics exposed in type area (fig. 2), measured bed by bed by using a Jacob staff. Note stratigraphic position of new $^{40}Ar/^{39}Ar$ radiometric age reported in this study.

Figure 13. Lithic-tuff-breccia facies (pyroclastic-flow deposits) in the Mount Galen Volcanics at Mount Galen (fig. 2). Outcrop represents approximately 210–220-m interval in stratigraphic column (fig. 12).

rocks of Foraker Glacier and Mount Galen Volcanics have different K_2O, Al_2O_3, and MgO trends with respect to SiO_2 (fig. 14).

All of the samples from each suite of rocks exhibit some degree of light-rare-earth-element (LREE) enrichment (fig. 15). Foraker Glacier rhyolites show greater LREE enrichment than do Foraker Glacier basalts, and one sample (FGW97–19, tables 2, 3) of Foraker Glacier basalt shows an exceptionally low LREE enrichment (fig. 15). Foraker Glacier rhyolites display a marked negative Eu anomaly. Samples of Mount Galen basalt and andesite vary widely in rare-earth-element contents and display a marked positive Eu anomaly (fig. 15). Samples of Mount Galen dacite and rhyolite are more uniform in rare-earth-element contents than are the basalts. Mount Galen dacites and rhyolites are not as enriched in LREEs as are Foraker Glacier rhyolites.

A comparison of trace-element contents using chondrite-normalized spider diagrams reveals some important differences between the volcanic rocks of Foraker Glacier and the Mount Galen Volcanics (fig. 16). The volcanic rocks of Foraker Glacier show a marked increase in Rb, Th, and K contents from the basalt to the rhyolite samples. For example, average Rb/Ba ratios for Foraker Glacier basalts and basaltic andesites, andesites, and rhyolites are 0.02, 0.1, and 1.3, respectively. The Mount Galen Volcanics does not show the same systematic strong increases in Rb, Th, and K contents between the mafic and felsic end members. (Average Rb/Ba ratios for Oligocene basalts and basaltic andesites, andesites, and dacites and rhyolites are 0.03, 0.09, and 0.05, respectively.) Another significant trace-element pattern is the systematic large decrease in Sr, P, and Ti contents between Foraker Glacier basalts, andesites, and rhyolites. In contrast, the Mount Galen Volcanics is enriched in Sr (especially the basalts and andesites) and shows smaller decreases in P and Ti contents from the mafic to felsic end members (fig. 16). Also, the Mount Galen basaltic through felsic samples show a pronounced Nb-Ta-depletion trend that is absent in Foraker Glacier basalts and is only subtly expressed in Foraker Glacier andesites and rhyolites.

The geochemical data reveal different petrogenetic histories for the volcanic rocks of Foraker Glacier and the Mount Galen Volcanics. The volcanic rocks of Foraker Glacier were probably derived from a slightly depleted subcontinental lithospheric mantle source with some characteristics of subduction magmatism. Basalt sample FGW97–19 (tables 2, 3), from the stratigraphically lowest lava, is the most primitive sample from the volcanic rocks of Foraker Glacier and represents the least

Table 2. Major-element composition of samples from the volcanic rocks of Foraker Glacier and the Mount Galen Volcanics.

[X-ray-fluorescence analyses in weight percent by Chemex Laboratories, Inc. LOI, loss on ignition]

Sample	SiO_2	Na_2O	K_2O	Al_2O_3	MgO	Fe_2O_3	CaO	MnO	TiO_2	P_2O_5	LOI	Total
Volcanic rocks of Foraker Glacier (late Paleocene and early Eocene)												
FGW97–19	47.93	3.30	0.32	15.54	5.98	10.21	4.86	0.11	1.90	0.16	7.59	97.90
FGW97–140	50.94	2.48	1.39	14.64	4.74	8.85	8.05	.15	1.55	.39	5.56	98.74
FGW97–121	51.94	2.29	.38	15.52	4.03	9.07	7.64	.13	1.59	.37	6.00	98.96
FGW97–189.5	54.30	2.15	1.10	15.44	3.82	7.97	5.99	.12	1.58	.38	5.19	98.04
FGW97–154	55.81	2.14	1.56	14.58	3.99	8.19	6.25	.11	1.56	.33	5.04	99.56
FGW97–85	59.88	2.43	3.89	15.41	2.93	6.92	3.57	.10	1.24	.28	3.79	100.44
FGW97–46	60.76	3.20	3.83	14.62	2.35	6.16	3.11	.10	1.20	.26	4.53	100.12
FGW–1	71.76	2.18	5.79	12.22	.23	1.90	.31	.02	.10	.02	5.40	99.92
FGW–3	72.84	3.34	5.60	12.72	.10	.86	.43	– – –	.12	.08	3.89	99.96
FGW–6	74.59	3.67	5.59	12.69	.16	1.45	.55	.03	.12	.04	1.05	99.94
FGW–7f	75.47	2.79	6.81	11.96	.35	1.49	.34	.03	.10	.09	.60	100.02
FGW97–291	77.91	2.52	5.23	12.44	.05	1.29	.63	<.01	.14	.01	.86	101.08
FGW97–345	78.43	1.89	6.26	12.14	.04	1.02	.16	.01	.13	.01	.82	100.91
FGW97–267	78.94	2.27	5.30	12.21	.08	1.17	.13	.01	.12	.01	1.01	101.25
Mount Galen Volcanics (late Eocene and early Oligocene)												
Muldrow Glacier area												
MG1–220bc	53.72	3.66	1.14	16.96	3.67	7.75	8.10	0.11	1.58	0.20	2.30	99.19
MG1–18a	57.16	1.62	3.91	14.23	2.47	5.20	7.23	.19	.67	.26	7.80	100.74
MG1–47.3	57.34	3.17	1.37	18.96	.45	8.76	6.49	.05	1.75	.05	.75	99.14
MG1–18	59.47	.28	3.71	13.33	2.99	4.99	6.89	.19	.66	.16	6.16	98.83
MG1–220GC	61.45	3.22	2.08	17.26	1.93	4.41	4.86	.10	.58	.18	2.80	98.87
MG1–40	64.81	2.07	5.41	14.17	.29	1.11	1.91	.02	.11	.10	8.65	98.66
MG1–220dc	70.67	3.49	2.77	15.09	.91	2.56	2.09	.05	.30	.08	1.25	99.26
MG1–28.5	72.18	3.33	2.80	13.66	.52	3.05	1.69	.05	.28	.04	3.81	101.41
MG1–86C1	75.99	2.56	2.37	12.41	1.03	2.87	.18	.04	.33	.05	2.59	100.42
Mount Galen type area												
GA1–46	52.73	3.09	1.33	18.82	3.06	8.90	7.52	0.24	1.25	0.20	1.88	99.02
GA1–31	53.99	3.39	1.30	18.45	2.22	8.13	7.41	.25	1.31	.18	1.81	98.44
GA1–33	54.49	3.21	1.26	20.22	2.11	9.12	8.30	.19	1.29	.35	.42	100.96
GA1–123	59.83	3.40	1.04	17.81	2.06	4.23	5.04	.10	.67	.12	5.01	99.31
GA1–148.3	63.58	3.51	1.56	15.97	1.77	4.06	4.32	.08	.66	.19	3.88	99.58
GA1–100	65.28	3.76	2.19	17.23	.60	3.04	4.47	.03	.72	.14	1.72	99.18
GA1–225C	65.76	2.36	1.64	17.45	1.64	6.24	4.71	.11	.81	.05	.42	101.17
GA1–96.5	68.25	3.90	2.13	16.56	.70	2.71	4.35	.03	.79	.15	1.69	101.26
Mount Galen data from Decker and Gilbert (1978)												
1b	46.00	3.40	1.10	17.00	5.00	5.80	8.20	0.04	3.00	0.35	– – –	89.89
2	47.00	3.80	1.20	17.00	4.40	5.30	8.10	.21	2.90	.45	– – –	90.36
6	58.60	3.20	.84	17.20	2.80	4.30	5.90	.04	.75	.09	– – –	93.72
5	59.20	3.10	.96	17.20	3.60	2.50	5.70	.05	.90	.10	– – –	93.31
4	61.50	4.20	1.60	18.10	2.40	1.60	6.00	.18	.90	.15	– – –	96.63
3	63.20	3.80	1.90	16.60	2.10	3.60	5.40	.09	.66	.10	– – –	97.45
7	64.80	3.60	2.20	15.70	1.70	4.00	4.10	.84	.46	.08	– – –	97.48
8	69.00	3.60	2.30	15.50	1.30	3.00	3.80	.77	.46	.10	– – –	99.83

Table 3. Trace-element composition of samples from the volcanic rocks of Foraker Glacier and the Mount Galen Volcanics.

[Inductively coupled plasma mass-spectrometric analyses in parts per million by Chemex Laboratories, Inc.]

Sample	Ba	Ce	Dy	Er	Eu	Gd	Hf	Ho	La	Lu	Nb	Nd	Pr	Rb	Sm	Sr	Ta	Tb	Th	Tm	Y	Yb	Zr
Volcanic rocks of Foraker Glacier (late Paleocene and early Eocene)																							
FGW97–19	477	20.5	3.8	2.5	1.1	3.9	4	0.9	9	0.4	8	13.5	3	5.2	3.4	307	0.9	0.7	1	0.4	24	2.6	159
FGW97–140	928	64	5.5	3.1	1.8	6.4	6	1.2	31	.4	21	30.5	7.6	24.6	6.4	415	2	1.1	7	.5	30.5	2.9	244
FGW97–121	432.5	50.5	4.7	2.9	1.4	5.9	4	.8	24	.4	16.7	26	6.3	5.8	5	512	.9	.8	4	.4	20.1	2.6	204
FGW97–189.5	747	66.5	5.5	3.4	2.1	6.7	7	1.2	32.5	.4	19	33	8.2	19.6	6.8	392	1	1	8	.4	35.5	3.3	277
FGW97–154	1,155	55.5	5.4	3	1.6	5.7	7	1.1	27	.5	18	27.5	6.8	36.2	6	466	1	.9	7	.4	30	3.1	255
FGW97–85	1,160	63	5.6	3.4	1.9	6.8	7	1.1	30	.4	15	31.5	7.7	103	7	275	1	.9	9	.5	32	3	248
FGW97–46	885	65.5	5.8	3.3	1.5	6.6	7	1.2	31	.5	16	32.5	8.1	115.5	7.2	212	1.5	1	11	.5	34.5	3.4	257
FGW–1	210	192.5	12.8	6.8	.5	16.2	8	2.6	86	1.1	43	75	21.3	259	13.9	14.9	9	2.4	20	.9	57.5	7	222
FGW97–291	184	155	8.8	5.3	.4	10.6	7	1.7	76.5	.8	22	66	17.6	236	12.1	15	2	1.7	25	.7	51.5	4.9	191
FGW97–345	214	143	7.5	4.1	.4	9.4	7	1.5	73	.6	20	59	16.2	279	9.9	14	2	1.3	24	.7	40.5	4.2	169.5
FGW97–267	206	108	6.7	4.2	.3	7.9	6	1.3	53.5	.6	19	45.5	12.5	242	8.7	14	1.5	1.2	20	.6	39.5	3.9	151
Mount Galen Volcanics (late Eocene and early Oligocene)																							
Muldrow Glacier area																							
MG1–220bc	443	22.5	4.4	2.6	1.4	4.3	3	0.8	10	0.4	7.6	14	3.1	16.3	3.4	290	0.5	0.6	2.8	0.3	23.8	2.6	160
MG1–47.3	556	9.5	2.1	1.9	1	1	3	.4	5.5	.3	7	4.5	1	19	.9	387	.4	.1	2	.3	17.5	2.4	160
MG1–18	403.5	25.5	2.7	1.9	1.1	3.4	.9	.5	11.5	.2	4.9	15	3.2	118	2.4	229	.3	.4	3	.1	12.3	1.6	81.5
MG1–220GC	974	39	2.8	1.7	1.3	4.1	3	.7	19.5	.3	7	17	4.9	42	3.9	547	1.5	.5	5	.3	14	2	108
MG1–40	741	67	6.1	4.2	.5	6.3	5	1.3	33	.7	14	29	7.8	108	5.8	106.5	3.5	1	9	.7	32	4.3	167
MG1–220dc	1,307	28	1	.7	.5	1.8	.9	.1	14.5	<.1	4.6	10	2.9	42.6	1.8	382	.35	.1	6.6	<.1	7.3	1	83
MG1–28.5	1,095	40.5	2.3	1.5	.6	2.9	4	.5	21.5	.3	7	15.5	4.5	62.2	3.4	417	.5	.4	8	.2	15	1.5	92.5
MG1–86C1	539	22.5	1.6	1.1	.3	1.5	3	.3	11	.2	5	8.5	2.6	71.4	1.7	295	.5	.2	5	.1	11.5	1.3	83.5
Mount Galen type area																							
GA1–46	755.2	22.5	2.3	1.6	1.2	3	1	0.4	11	0.1	6.8	13.5	3.1	17.2	2.5	900	0.45	0.3	2.6	0.1	13.8	1.7	100
GA1–31	680	22.5	2.9	1.7	1.5	3	3	.5	10.5	.3	5	13.5	3.2	20	3.5	1,000	.45	.4	2	.2	15	1.6	91
GA1–33	696	36.5	4.8	2.4	2.1	5.4	3	.8	17.5	.3	9	23	5.4	21.4	5.3	1,085	1.5	.7	3	.4	20.5	2.4	108
GA1–123	747.2	24.5	1.6	1	1.1	1.6	1	.2	13	.1	6.1	11.5	2.8	13.4	2	725	.35	.3	4.6	<.1	8.6	1.1	92.5
GA1–148.3	846	35.5	2.4	1.2	1.1	2.9	3	.4	17.5	.1	6	17.5	4.2	16.8	3.5	666	.4	.4	5	.1	12	1.1	108
GA1–100	1,117	31	1.7	.9	1.3	2.8	2	.2	16.5	<.1	6.4	14	3.6	38.9	2.8	609	.4	.3	6.2	<.1	8.3	.6	109
GA1–225C	891	39	2.6	1.5	1.3	3.7	3	.5	21	.3	8	19.5	4.7	22	4.1	598	2	.5	6	.2	12.5	1.7	106
GA1–96.5	1,000	35	2.1	1	1	2.8	3	.4	18.5	.1	6	16.5	4.2	43.6	3.2	635	.45	.4	5	.1	10	1	96.5

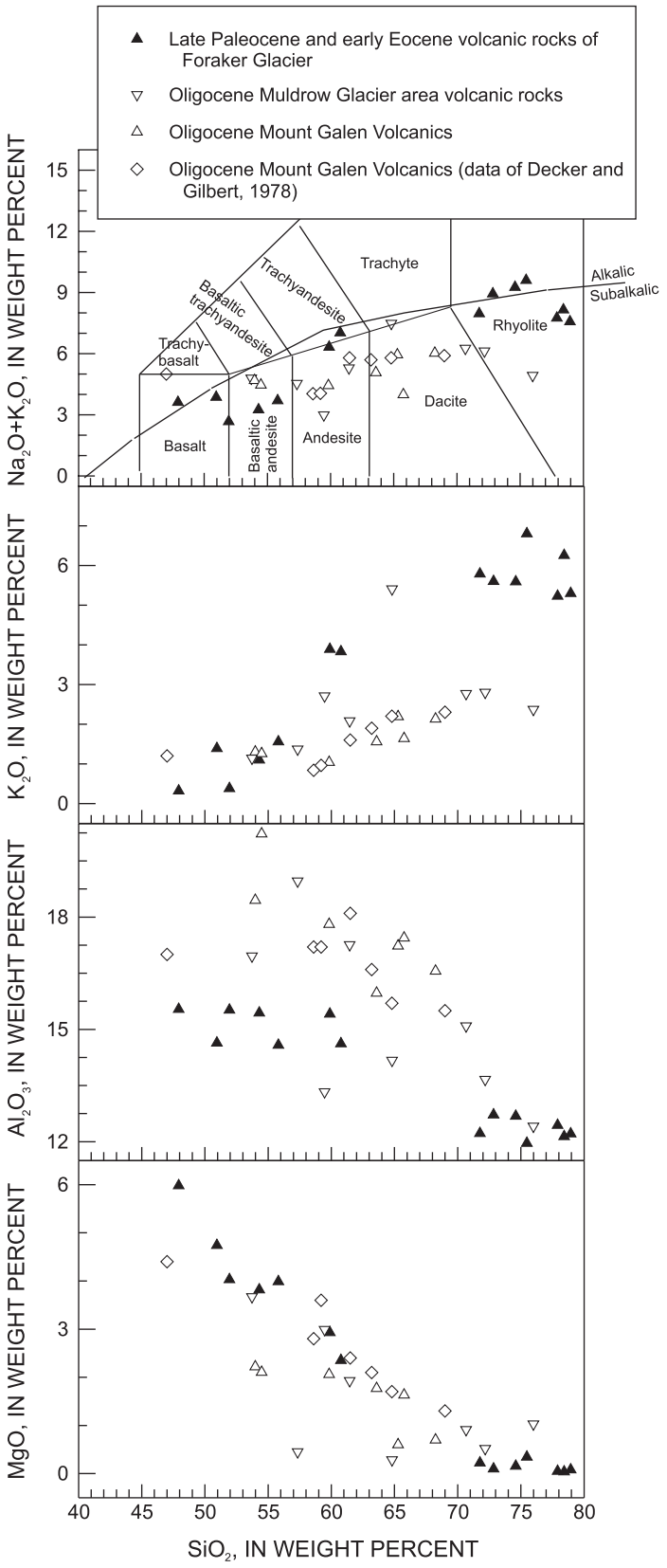

Figure 14. Major-element-variation diagrams for the volcanic rocks of Foraker Glacier and the Mount Galen Volcanics. Rock classifications after LeBas and others (1986).

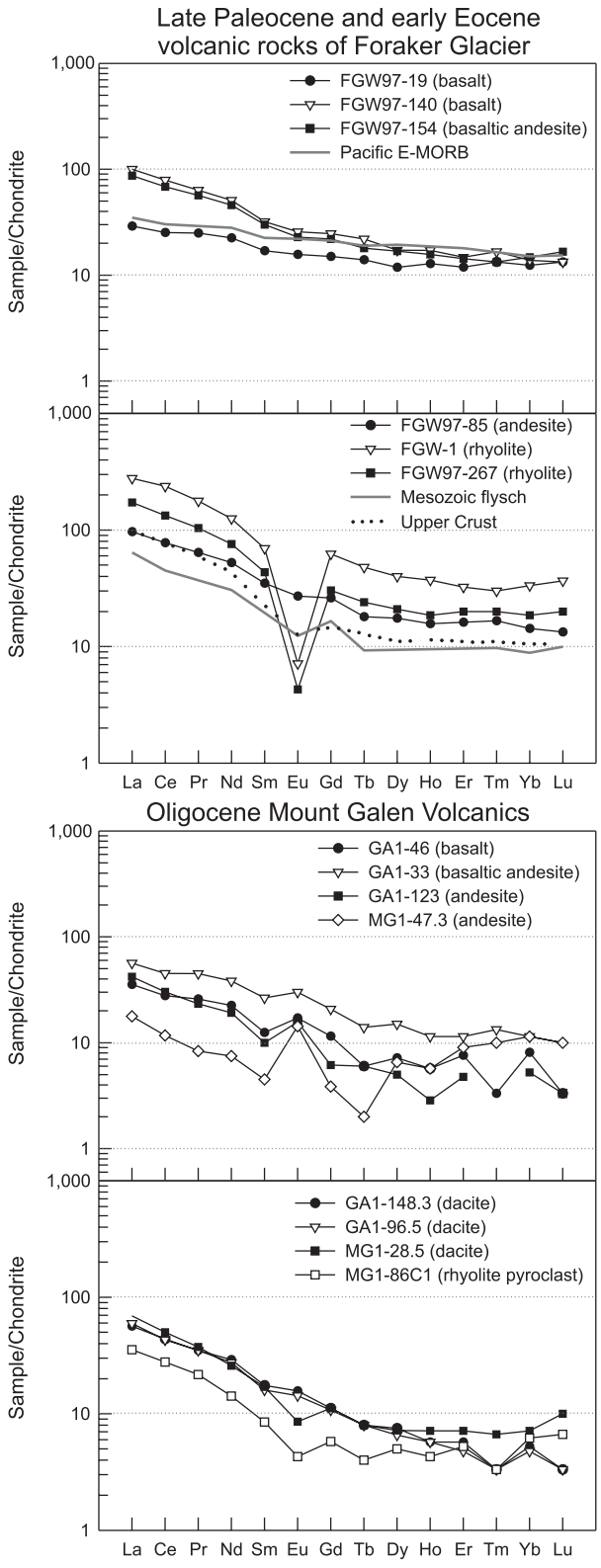

Figure 15. Chondrite-normalized rare-earth-element diagrams for samples of the volcanic rocks of Foraker Glacier and the Mount Galen Volcanics. Average compositions of Pacific enriched midoceanic-ridge basalt (E–MORB), Mesozoic flysch in the Mount McKinley area (fig. 2), and upper-crustal rocks from Klein and Langmuir (2000), Lanphere and Reed (1985), and Taylor and McLennan (1985), respectively; chondrite-normalizing values from Boynton (1984).

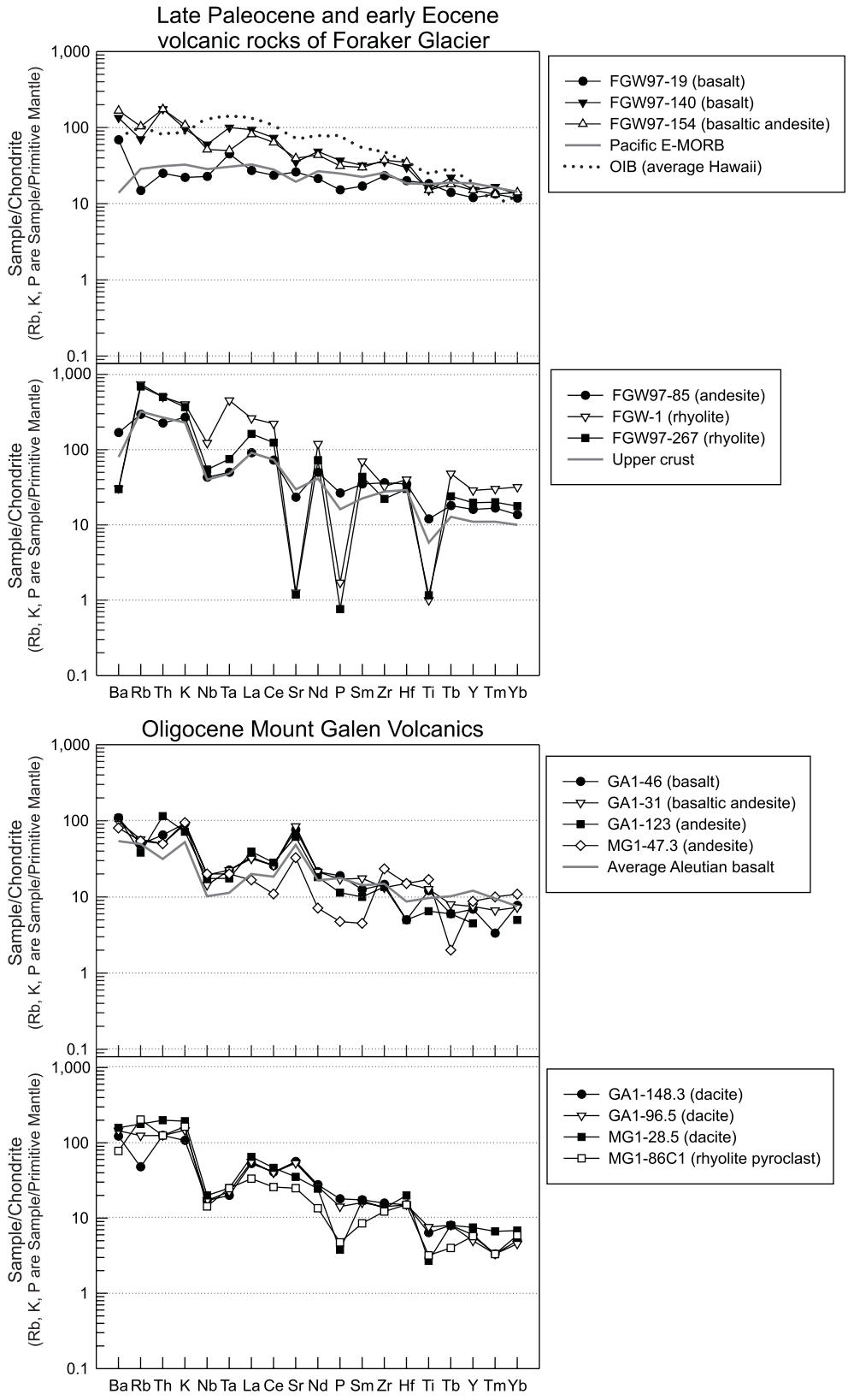

Figure 16. Normalized trace-element diagrams for samples of the volcanic rocks of Foraker Glacier and the Mount Galen Volcanics. Average compositions of Pacific enriched midoceanic-ridge basalt (E–MORB) from Klein and Langmuir (2000), of oceanic-island basalt (OIB) (Hawaii) from Spengler and Garcia (1988) and Sims and others (1999), of upper-crustal rocks from Taylor and McLennan (1985), and of Aleutian basalt from Kay and Kay (1994) and Fournelle and others (1994). Chondrite-normalizing values from Thompson and others (1984), and primitive-mantle-normalizing values from Sun (1980).

evolved magma for these rocks. This sample exhibits only slight LREE enrichment and low contents of the incompatible elements Rb, Th, and K (figs. 15, 16). The sample is similar in composition to enriched midoceanic-ridge basalts of the Pacific Ocean (E-MORB, fig. 16), with the notable exception of strongly elevated Ba content (fig. 16). Other Foraker Glacier basalts show more enriched trends than sample FGW97–19, with more LREE enrichment and higher Rb, Th, and K contents. These more enriched basalts are superficially similar to oceanic-island basalts (OIB, fig. 16), but the basalts of Foraker Glacier have higher La/Nb ratios than do oceanic-island basalts (OIB, fig. 17), suggesting that they did not form directly from asthenospheric mantle (Thompson and others, 1984; Fitton and others, 1988). Instead, the ranges of Zr/Nb and La/Nb ratios in Foraker Glacier basalts are similar to those in Miocene basalts derived from subduction-modified (hydrated) lithospheric-mantle sources beneath the Western United States (fig. 17; Fitton and others, 1988). The elevated Ba and Th contents of Foraker Glacier basalts also indicate the subduction-related processes whereby these elements become enriched in the lithospheric mantle wedge, possibly from subducted sedimentary rocks and the release of hydrous fluids from the downgoing slab (Kay, 1984; Thorpe and others, 1984). Foraker Glacier basalts and andesites also have high Ba/Ta ratios (464–1,160); according to Gill (1981) a Ba/Ta ratio of >450 is a key characteristic of subduction-related volcanic rocks. Foraker Glacier basalts and andesites do not, however, show elevated Sr contents, which are typical of subduction-related arc rocks (Wilson and Davidson, 1984).

Foraker Glacier rhyolites were most likely formed by partial melting and assimilation of crustal rocks and evolved partly by fractional crystallization. A systematic increase in La/Nb ratio from Foraker Glacier basalts to rhyolites is one indication of crustal contamination (fig. 18; Thompson and others, 1984). The rhyolites are strongly enriched in Rb, Th, and K, as well as in LREEs, and are similar in composition to average upper continental crust (fig. 16). In contrast to Foraker Glacier basalts and andesites, the rhyolites have very low Ba/Ta ratios (23–137), indicating that the rhyolites did not evolve directly from subduction magmas (for example, Gill, 1981). Instead, we interpret that the rhyolites were formed by partial melting of crustal rocks by the basaltic magmas and evolved by a combination of assimilation and fractional crystallization. Strong depletion of Sr, P, and Ti in the rhyolites indicates that fractional crystallization of plagioclase, apatite, and Fe-Ti oxides was important in their formation (fig. 16). The strong negative Eu anomaly in the rhyolites also supports fractional crystallization of plagioclase (fig. 15).

Mount Galen basalts and andesites have elevated Ba, Th, and Sr contents and a marked paired depletion of Nb and Ta (fig. 16), all common characteristics of subduction-related volcanic rocks (Kay, 1984; Wilson and Davidson, 1984; Thorpe and others, 1984). Overall, these rocks have a trace-element pattern that is nearly identical to that of average Aleutian Arc basalt (fig. 16). Mount Galen dacites and rhyolites are similar in geochemical affinity to the basalts and andesites and display enrichments in Rb, Th, and Sr, as well as a distinctive Nb-Ta trough (fig. 16). The dacites and rhyolites also show slight P and Ti depletion, indicating that they evolved partly by fractional crystallization. Except for one sample, the samples of the Mount Galen Volcanics have high Ba/Ta ratios of 446 to 3,734: Dacite tuff sample MG1–40 has a Ba/Ta ratio of 212. We interpret that the Mount Galen Volcanics was formed as typical subduction-related magmas where basalts were derived by partial melting of an enriched mantle wedge and that the more felsic magmas evolved mostly by fractional crystallization of the mafic magmas. The low Ba/Ta ratio of one dacite sample indicates that at least some of the felsic rocks were formed by partial melting and (or) assimilation of crustal rocks.

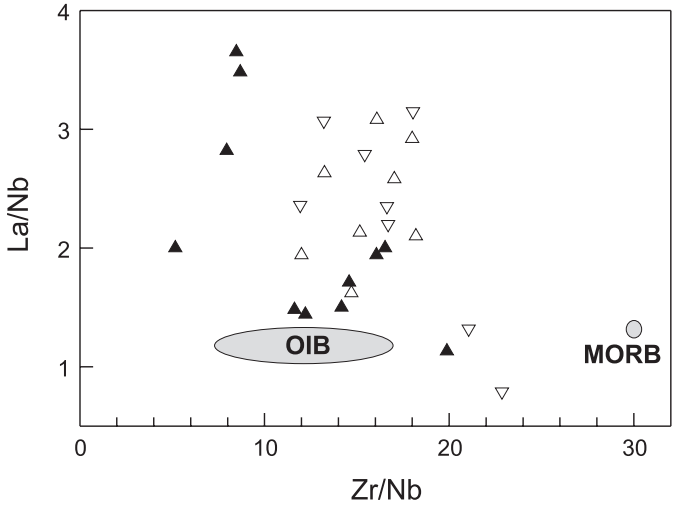

Figure 17. La/Nb versus Zr/Nb ratios in the volcanic rocks of Foraker Glacier and the Mount Galen Volcanics. Ranges for oceanic-island basalts (OIB) and midoceanic-ridge basalts (MORB) from Rollinson (1993, table 6.7). Same symbols as in figure 14.

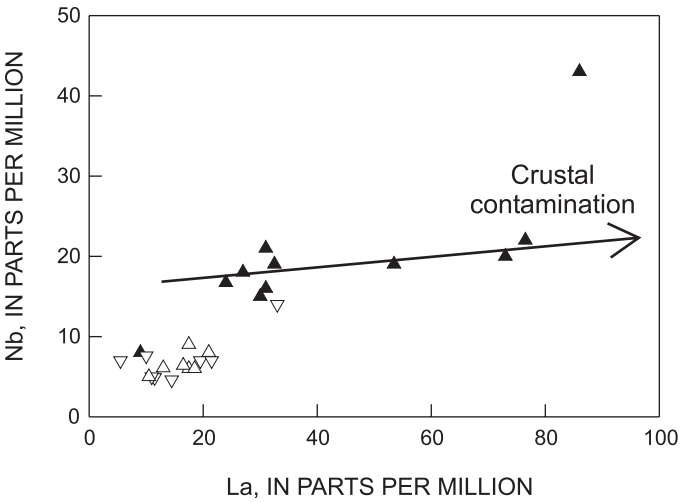

Figure 18. Nb versus La contents in the volcanic rocks of Foraker Glacier and the Mount Galen Volcanics. Same symbols as in figure 14.

Discussion

The volcanic and sedimentary rocks described above record an important sequence of tectonic events that shaped the ancestral Alaska Range. The sedimentary rocks that underlie the late Paleocene and early Eocene volcanic rocks of Foraker Glacier record an episode of tectonic uplift and basin subsidence. This uplift most likely coincided with an undetermined amount of shortening of the underlying layers of Paleozoic metamorphic rocks (fig. 4). The present-day orientation of metamorphic foliation implies that this shortening was in response to north-south compression, but more regional data are needed to evaluate shortening direction(s) and potential crustal rotations. Nevertheless, a significant point is that the metamorphic rocks of this region were uplifted and eroded to form the overlying synorogenic conglomerate. Although the timing of this uplift event is not yet precisely constrained, it preceded late Paleocene and early Eocene volcanism in the region. The Foraker Glacier synorogenic sedimentary deposits probably correlate with the lower part of the Cantwell Formation to the east in the Healy quadrangle, which also underlies late Paleocene and early Eocene volcanic rocks. The lower part of the Cantwell Formation in the Healy quadrangle was deposited along the leading edge of northward-vergent thrust sheets that formed in response to accretion of the Wrangellia composite terrane (Ridgway and others, 1997). By analogy, we propose that the Foraker Glacier synorogenic deposits also record uplift in response to accretion of the Wrangellia composite terrane and represent a westward extension of the Cantwell Basin (fig. 19*A*). If the Foraker Glacier synorogenic deposits are part of the lower part of the Cantwell Formation, then the lowermost conglomerate is the coarsest lower Cantwell deposit yet documented (maximum clast sizes, >2 m in diameter). The very coarse grain size indicates that the Foraker Glacier conglomerates represent deposition near an area of uplift of the ancestral Alaska Range. Paleoflow data for Foraker Glacier conglomerates reveal westward drainage, opposite to the eastward-flowing drainages documented by Ridgway and others (1997) for the lower part of the Cantwell Formation in the Healy quadrangle. These paleoflow data might indicate that the Cantwell Basin was "segmented" into different drainage systems which could have formed adjacent to separate regions of uplift (fig. 19*A*). The Foraker Glacier synorogenic sedimentary rocks were then uplifted, as indicated by the angular unconformity between them and the overlying volcanic rocks (fig. 4). This unconformity, which is analogous to the contact between the lower and upper parts of the Cantwell Formation in the Healy quadrangle, most likely represents the final stage of compression due to suturing of the Wrangellia composite terrane (Cole and others, 1999).

Magmatism associated with the Alaska Range belt of Wallace and Engebretson (1984) or the Alaska Range-Talkeetna Mountains belt of Moll-Stalcup (1994) was occurring predominantly south of the Foraker Glacier area during the episode of synorogenic sedimentation. The latest phase of this magmatism is represented in the study area by the 55- to 60-Ma McKinley sequence plutons and the volcanic rocks of Foraker Glacier. These younger igneous rocks are geochemically distinct from older (60–72 Ma) rocks of the magmatic belt (generally higher K_2O, lower Al_2O_3, lower Sr, and higher Nb contents; Lanphere and Reed, 1985; Moll-Stalcup, 1994). Also, as shown in this chapter, the volcanic rocks of Foraker Glacier differ from rocks with "typical" subduction-related geochemical affinities. The volcanic rocks of Foraker Glacier and, by association, the other 55- to 60-Ma rocks in the belt most likely represent changes in the style of subduction magmatism caused by accretion of the Wrangellia composite terrane and the ensuing southward shift in the subduction zone (Wallace and Engebretson, 1984; Scholl and others, 1986). Coeval mafic magmas could have formed by partial melting of a remnant subduction-related mantle wedge, but Foraker Glacier basalts (especially sample FGW97–19, tables 2, 3) are more depleted in incompatible elements than would be expected for arc basalts. Reiners and others (1996) documented gabbro xenoliths in Alaska Range plutons with typical depleted-mantle isotopic compositions; they proposed that the Alaska Range plutons ultimately had a depleted mantle source of primary magmas which then evolved by several processes of partial assimilation and fractional crystallization. Our results, in combination with the those of Reiners and others (1996), imply that if a subduction-related mantle wedge was a source of primary magmas for these rocks, then it was more depleted than would be predicted for continental-margin arcs (for example, Pearce and Parkinson, 1993). One possible source of depleted primary magmas could have been related to early Tertiary spreading-ridge subduction beneath southern Alaska (for example, Sisson and Pavlis, 1993; Bradley and others, 1993). In this scenario, a depleted mantle-slab window could have formed beneath south-central Alaska as the spreading ridge was consumed—a hypothesis that has been proposed to explain the origin of plutons along the south coast of Alaska (Bradley and others, 1993) but has not yet been tested for early Tertiary volcanism in interior Alaska. We neither support nor refute the ridge-subduction hypothesis at this time but merely present it to provide a more regional perspective of magmatic and tectonic events.

The felsic magmas that were erupted to form the Foraker Glacier rhyolites were derived by melting of crustal rocks and evolved partly by fractional crystallization. Two sets of crustal rocks in the region that could have been involved in the formation of the felsic magmas are Paleozoic metamorphic rocks and the Mesozoic Kahiltna assemblage flysch (fig. 2). On the basis of geochemical evidence, Lanphere and Reed (1985) and Reiners and others (1996) suggested that early Tertiary granitic rocks of the Alaska Range were formed by melting of the Kahiltna flysch. In particular, Reiners and others (1996) proposed that melting of the Kahiltna flysch was probably induced by an early stage of mica dehydration of the flysch caused by intrusion of mantle-derived mafic magmas. Foraker Glacier rhyolites are more enriched in rare-earth elements than is the Kahiltna flysch and are more similar in composition to average upper-crustal rocks (figs. 15, 16). Whereas partial melting and (or) assimilation of the Kahiltna flysch may have been involved in the formation of Foraker rhyolites, our data suggest

that other, more enriched crustal sources were involved as well. In a study of Tertiary granitic rocks to the northeast of our study area (in the Yukon-Tanana terrane), Aleinikoff and others (2000) ruled out flysch as a likely source and proposed that the felsic magmas were derived from partial melting of Paleozoic rocks. Foraker Glacier rhyolites may reflect a mixed crustal component in which some combination of Paleozoic rocks and Mesozoic flysch was involved in forming felsic magmas; additional geochemical work on these rocks, especially isotopic analyses, is needed to test this hypothesis.

The geochemical and age data reveal that the volcanic rocks of Foraker Glacier were comagmatic with Cantwell volcanic rocks of the Healy quadrangle (Cole, 1998; Cole and others, 2000). Paleoflow data from volcanic conglomerate interbedded in the lower part of the volcanic rocks of Foraker Glacier show eastward transport away from a probable eruptive center. Eastward paleoflow directions were also recorded in volcanic conglomerates of the Healy quadrangle (fig. 19*B*; Slaugenhoup and others, 1997; Cole and others, 1999). We interpret that these late Paleocene and early Eocene volcanic

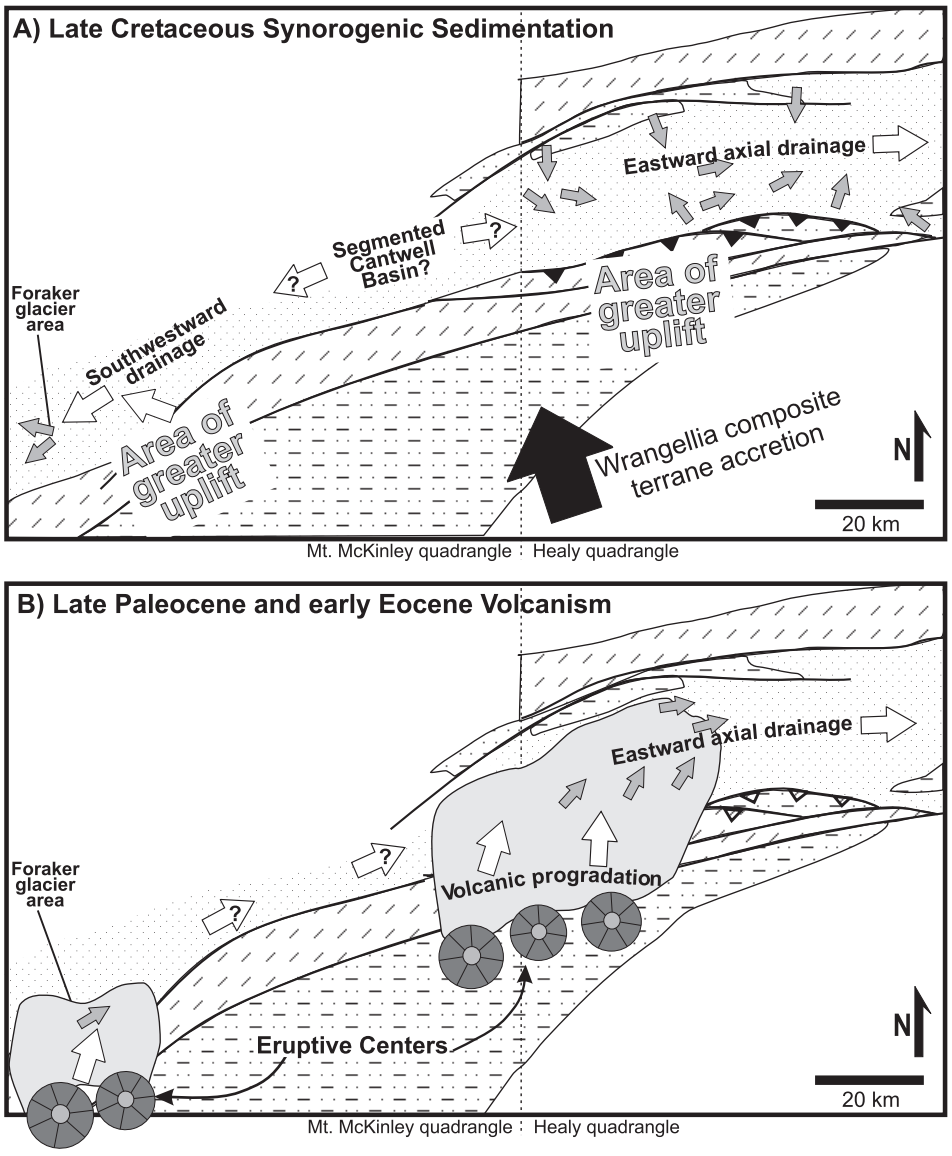

Figure 19. Paleogeographic cartoons showing inferred Late Cretaceous drainage systems (*A*) and late Paleocene and early Eocene volcanic centers (*B*) in the Cantwell Basin. Stippling, sedimentary rocks in lower part of the Cantwell Formation; gray shading, volcanic rocks in upper part of the Cantwell Formation. Gray arrows denote measured paleoflow directions; white arrows denote inferred drainage directions. Paleoflow data for the Healy quadrangle from the following sources: lower part of the Cantwell Formation, Trop (1996) and Ridgway and others (1997); upper part of the Cantwell Formation, Slaugenhoup and others (1997) and R.B. Cole (unpub. data). Paleoflow data shown for the Mount McKinley quadrangle are reported in text. Same map symbols as in figure 2.

rocks (both in the Foraker Glacier area and in the Healy quadrangle) were most likely erupted from multiple ventsites close to the southern margin of the Cantwell Basin. During early stages of volcanism, fluvial deposystems drained from the ventsites into the Cantwell Basin and then flowed eastward along the central part of the basin (fig. 19*B*). During later stages of volcanism, primary volcanic rocks prograded into and filled the Cantwell Basin.

The Mount Galen Volcanics displays a geochemical pattern that is typical of arc rocks related to subduction processes. These rocks were most probably erupted along the north end of the Alaska-Aleutian subduction-related magmatic belt of Wallace and Engebretson (1984), which crosscut late Paleocene and early Eocene rocks in the study area. The Oligocene plutons in the region (Foraker, McGonnagal, and Eielson plutons) are also considered to be part of this magmatic belt (Reed and Lanphere, 1974; Decker and Gilbert, 1978; Moll-Stalcup, 1994).

Conclusions

1. Two episodes of Tertiary magmatism are recorded in the southern part of the Mount McKinley 1:250,000-scale quadrangle. (i) A late Paleocene and early Eocene episode occurred after tectonic uplift and accretion of the Wrangellia composite terrane to southern Alaska. The volcanic rocks exhibit some of the characteristics of typical subduction-related arc rocks, but the primary magmas were more depleted than were magmas formed from enriched mantle sources. Their petrogenesis was most likely influenced by processes associated with accretion of the Wrangellia composite terrane where the magmas may have been partly derived from a modified (relatively depleted) remnant subduction-related mantle wedge or may have been related to a depleted mantle-slab window that formed during early Tertiary ridge subduction beneath southern Alaska. (ii) A late Eocene and early Oligocene episode of magmatism produced volcanic rocks that exhibit geochemical characteristics which are typical of subduction-related arc rocks and are most likely a northward extension of the Aleutian-Alaska magmatic belt of Wallace and Engebretson (1984).
2. Before the late Paleocene and early Eocene magmatic event was a period of tectonic uplift during which Paleozoic metamorphic rocks were folded. Part of this shortening most likely occurred in response to north-south compression caused by accretion of the Wrangellia composite terrane. As a result of this uplift, cobble-boulder synorogenic conglomerate was deposited unconformably over the Paleozoic metamorphic rocks. The conglomerate fines upward into mostly sandstone and shale that record a period of basin subsidence before the onset of late Paleocene and early Eocene volcanism. These sedimentary strata are most likely equivalent to the lower part of the Cantwell Formation in the Healy quadrangle and represent a westward extension of the Cantwell Basin.

Acknowledgments

The field research for this project was initiated with helicopter and base-camp support by the U.S. Geological Survey; subsequent fieldwork was supported by grants to Ronald Cole from the donors of the Petroleum Research Fund, administered by the American Chemical Society, and from the National Science Foundation. We thank Phil Brease of Denali National Park and Preserve for field and permit support to conduct the fieldwork. Garret Slaugenhoup, Chris Turner, and Michael Walker provided field assistance. Alison Till, Dwight Bradley, and Steve Nelson provided discussions about the rocks in the Mount McKinley quadrangle. Dwight Bradley, Steve Nelson, and Ric Wilson reviewed the manuscript.

References Cited

Aleinikoff, J.N., Farmer, G.L., Rye, R.O., and Nokleberg, W.J., 2000, Isotopic evidence for the sources of Cretaceous and Tertiary granitic rocks, east-central Alaska—implications for the tectonic evolution of the Yukon-Tanana Terrane: Canadian Journal of Earth Sciences, v. 37, no. 6, p. 945–956.

Allen, P.A., 1981, Sediments and processes on a small stream-flow dominated, Devonian alluvial fan, Shetland Islands: Sedimentary Geology, v. 29, no. 1, p. 31–66.

Boynton, W.V., 1984, Geochemistry of the rare earth elements—meteorite studies, *in* Henderson, Paul, ed., Rare earth element geochemistry: Amsterdam, Elsevier, p. 63–114.

Bradley, D.C., Haeussler, P.J., and Kusky, T.M., 1993, Timing of Early Tertiary ridge subduction in southern Alaska, *in* Dusel-Bacon, Cynthia, and Till, A.B., eds., Geologic studies in Alaska by the U.S. Geological Survey, 1992: U.S. Geological Survey Bulletin 2068, p. 163–177.

Cas, R.A.F., and Wright, J.V., 1987, Volcanic successions—modern and ancient: London, Allen and Unwin, 528 p.

Cole, R.B., 1998, Early Tertiary post-subduction volcanism and deformation along the north side of the McKinley fault, Alaska: Geological Society of America Abstracts with Programs, v. 30, no. 7, p. 177.

Cole, R.B., and DeCelles, P.G., 1991, Subaerial to submarine transitions in early Miocene pyroclastic flow deposits, southern San Joaquin basin, California: Geological Society of America Bulletin, v. 103, no. 2, p. 221–235.

Cole, R.B., Hooks, Benjamin, Turner, Christopher, and Slaugenhoup, Garret, 2000, Unroofing of metamorphic terranes and subsequent volcanism—Late Cretaceous(?)-early Tertiary basin evolution along the McKinley fault, McKinley 1°×3° quadrangle, Alaska [abs.]: Geological Society of America Abstracts with Programs, v. 32, p. A11.

Cole, R.B., Ridgway, K.D., Layer, P.W., and Drake, Jeffrey, 1999, Kinematics of basin development during the transition from terrane accretion to strike-slip tectonics, Late Cretaceous-early Tertiary Cantwell Formation, south central Alaska: Tectonics, v. 18, no. 6, p. 1224–1244.

Costa, J.E., 1988, Rheologic, geomorphic, and sedimentologic differentiation of water floods, hyperconcentrated flows, and debris flows, *in* Baker, V.R., Kochel, R.C., and Patton, P.C., eds., Flood geomorphology: New York, Wiley, p. 113–122.

Csejtey, Bela, Jr., Mullen, M.W., Cox, D.P., and Stricker, G.D., 1992, Geology and geochronology of the Healy quadrangle, south-central Alaska: U.S. Geological Survey Miscellaneous Investigation Series Map I–1961, scale 1:250,000.

Dalrymple, G.B., 1979, Critical tables for conversion of K-Ar ages from old to new constraints: Geology, v. 7, no. 11, p. 558–560.

DeCelles, P.G., Gray, M.B., Ridgway, K.D., Cole, R.B., Srivastava, Praveen, Pequera, Nuria, and Pivnik, D.A., 1991, Kinematic history of a foreland uplift from Paleocene synorogenic conglomerate, Beartooth Range Wyoming and Montana: Geological Society of America Bulletin, v. 103, no. 11, p. 1458–1475.

Decker, J.E., and Gilbert, W.G., 1978, The Mount Galen volcanics—a new middle Tertiary volcanic formation in the central Alaska Range: Alaska Division of Geological and Geophysical Surveys Geologic Report 59, 11 p.

Fisher, R.V., 1979, Models for pyroclastic surges and pyroclastic flows: Journal of Volcanology and Geothermal Research, v. 6, no. 3–4, p. 305–318.

Fisher, R.V., and Schmincke, H.-U., 1984, Pyroclastic rocks: Berlin, Springer-Verlag, 472 p.

Fitton, J.G., James, D., Kempton, P.D., Ormerod, D.S., and Leeman, W.P., 1988, The role of lithospheric mantle in the generation of late Cenozoic basic magmas in the western United States, *in* Menzies, M.A., and Cox, K.G., eds., Oceanic and continental lithosphere—similarities and differences: Oxford, U.K., Clarendon Press, p. 331–349.

Fournelle, J.H., Marsh, B.D., and Myers, J.D., 1994, Age, character, and significance of Aleutian arc volcanism, *in* Plafker, George, and Berg, H.C., eds., The geology of Alaska, v. G–1 *of* The geology of North America: Boulder, Colo., Geological Society of America, p. 723–757.

Gill, J.B., 1981, Orogenic andesites and plate tectonics: New York, Springer-Verlag, 390 p.

Kay, R.W., 1984, Elemental abundances relevant to identification of magma sources: Royal Society of London Philosophical Transactions, ser. A, v. 310, no. 1514, p. 535–547.

Kay, S.M., and Kay, R.W., 1994, Aleutian magmas in space and time, *in* Plafker, George, and Berg, H.C., eds., The geology of Alaska, v. G–1 *of* The geology of North America: Boulder, Colo., Geological Society of America, p. 687–722.

Klein, E.M., and Langmuir, C.H., 2000, GERM [Geochemical Earth Reference Model] MORB data by ocean basin, depth, and MORB type: URL http://EarthRef.org/GERM/data/klein/MORB_ocean.htm.

Lanphere, M.A., and Reed, B.L., 1985, The McKinley sequence of granitic rocks; A key element in the accretionary history of southern Alaska: Journal of Geophysical Research, v. 90, no. B13, p. 11413–11430.

LeBas, M.J., Maitre, R.W., Streckeisen, A.L., and Zanettin, B.A., 1986, Chemical classification of volcanic rocks based on the total alkali-silica diagram: Journal of Petrology, v. 27, no. 3, p. 745–750.

Lowe, D.R., 1982, Sediment gravity flows; II, Depositional models with special reference to the deposits of high-density turbidity currents: Journal of Sedimentary Petrology, v. 52, no. 1, p. 279–297.

McClelland, W.C., Gehrels, G.E., and Saleeby, J.B., 1992, Upper Jurassic-Lower Cretaceous basinal strata along the Cordilleran margin—implications for the accretionary history of the Alexander-Wrangellia-Peninsular terrane: Tectonics, v. 11, no. 4, p. 823–835.

Miall, A.D., 1977, A review of the braided-river depositional environment: Earth-Science Reviews, v. 13, no. 1, p. 1–62.

Moll-Stalcup, E.J., 1994, Latest Cretaceous and Cenozoic magmatism in mainland Alaska, *in* Plafker, George, and Berg, H.C., eds., The geology of Alaska, v. G–1 *of* The geology of North America: Boulder, Colo., Geological Society of America, p. 589–619.

Moll-Stalcup, E.J., Brew, D.A., and Vallier, T.L., 1994, Latest Cretaceous and Cenozoic magmatic rocks of Alaska, pl. 5 *of* Plafker, George, and Berg, H.C., eds., The geology of Alaska, v. G–1 *of* The geology of North America: Boulder, Colo., Geological Society of America, scale 1:2,500,000.

Nemec, Wojciech, and Steel, R.J., 1984, Alluvial and coastal conglomerates—their significant features and some comments on gravely mass-flow deposits, *in* Koster, E.H., and Steel, R.J., eds., Sedimentology of gravels and conglomerates: Canadian Society of Petroleum Geologists Memoir 10, p. 1–31.

Nokleberg, W.J., Plafker, George, and Wilson, F.H., 1994, Geology of south-central Alaska, *in* Plafker, George, and Berg. H.C., eds., The geology of Alaska, v. G–1 *of* The geology of North America: Boulder, Colo., Geological Society of America, p. 311–366.

Pearce, J.A., and Parkinson, I.J., 1993, Trace element models for mantle melting—application to volcanic arc petrogenesis, *in* Prichard, H.M., Alabaster, Tony, Harris, N.B.W., and Neary, C.R., eds., Magmatic processes and plate tectonics: Geological Society of London Special Publication 76, p. 373–403.

Pierson, T.C., and Scott, K.M., 1985, Downstream dilution of a lahar—transition from debris flow to hyperconcentrated streamflow: Water Resources Research, v. 21, no. 10, p. 1511–1524.

Plafker, George, Moore, J.C., and Winkler, G.R., 1994, Geology of the southern Alaska margin, *in* Plafker, George, and Berg, H.C., eds., The geology of Alaska, v. G–1 *of* The geology of North America: Boulder, Colo., Geological Society of America, p. 389–449.

Reed, B.L., and Lanphere, M.A., 1974, Offset plutons and history of movement along the McKinley segment of the Denali fault system, Alaska: Geological Society of America Bulletin, v. 85, no. 12, p. 1883–1892.

Reed, B.L., and Nelson, S.W., 1980, Geologic map of the Talkeetna quadrangle, Alaska: U.S. Geological Survey Miscellaneous Investigation Series Map I–1174, scale 1:250,000.

Reed, J.C., 1933, The Mount Eielson district, Alaska: U.S. Geological Survey Bulletin 849–D, p. 231–287.

Reed, J.C., Jr., 1961, Geology of the Mount McKinley quadrangle, Alaska: U.S. Geological Survey Bulletin 1108–A, 36 p., scale 1: 250,000.

Reiners, P.W., Nelson, B.K., and Nelson, S.W., 1996, Evidence for multiple mechanisms of crustal contamination of magma from compositionally zoned plutons and associated ultramafic intrusions of the Alaska Range: Journal of Petrology, v. 37, no. 2, p. 261–292.

Ridgway, K.D., Trop, J.M., and Sweet, A.R., 1997, Thrust-top basin formation along a suture zone, Cantwell Basin, Alaska Range—implications for development of the Denali fault system: Geological Society of America Bulletin, v. 109, no. 5, p. 505–523.

Rollinson, H.R., 1993, Using geochemical data—evaluation, presentation, interpretation: Essex, U.K., Longman Scientific & Technical, 352 p.

Rust, B.R., 1972, Structure and process in a braided river: Sedimentology, v. 18, no. 3–4, p. 221–245.

Scholl, D.W., Vallier, T.L., and Stevenson, A.J., 1986, Geologic evolution and petroleum geology of the Aleutian Ridge, *in* Scholl, D.W., Grantz, Arthur, and Vedder, J.G., eds., Geology and resource potential of the continental margin of western North America

and adjacent ocean basins; Beaufort Sea to Baja California (Earth Science Series, v. 6): Houston, Tex., Circum-Pacific Council for Energy and Mineral Resources, p. 123–155.

Sims, K.W.W., DePaolo, D.J., Murrell, M.T., Baldridge, W.S., Goldstein, S.L., Clague, D.A., and Jull, M., 1999, Porosity of the melting zone and variations in the solid mantle upwelling rate beneath Hawaii; inferences from ^{238}U-^{230}Th-^{226}Ra and ^{235}U-^{231}Pb disequilibria: Geochimica et Cosmochimica Acta, v. 63, no. 23–24, p. 4119–4138.

Sisson, V.B., and Pavlis, T.L., 1993, Geologic consequences of plate reorganization—an example from the Eocene Southern Alaska fore arc: Geology, v. 21, no. 10, p. 913–916.

Slaugenhoup, G.L., Cole, R.B., and Ridgway, K.D., 1997, Change from terrane accretion to volcanism along the McKinley fault as recorded by conglomerate of the Cretaceous-Eocene Cantwell Basin, south-central Alaska [abs.]: Geological Society of America Abstracts with Programs, v. 29, no. 1, p. 80.

Smith, G.A., 1986, Coarse-grained nonmarine volcaniclastic sediment—terminology and depositional process: Geological Society of America Bulletin, v. 97, no. 1, p. 1–10.

Sparks, R.S.J., 1976, Grain size variations in ignimbrites and implications for the transport of pyroclastic flows: Sedimentology, v. 23, no. 2, p. 147–188.

Sparks, R.S.J., Self, Stephen, and Walker, G.P.L., 1973, Products of ignimbrite eruptions: Geology, v. 1, no. 3, p. 115–118.

Spengler, S.R., and Garcia, M.O., 1988, Geochemistry of the Hawi lavas, Kohala Volcano, Hawaii: Contributions to Mineralogy and Petrology v. 99, no. 1, p. 90–104

Steiger, R.H., and Jäger, Emilie, compilers, 1977, Subcommission on geochronology—convention on the use of decay constants in geo- and cosmochronology: Earth and Planetary Science Letters, v. 36, no. 3, p. 359–362.

Stone, D.B., Panuska, B.C., and Packer, D.R., 1982, Paleolatitudes versus time for southern Alaska: Journal of Geophysical Research, v. 87, no. B5, p. 3697–3707.

Sun, S.-S., 1980, Lead isotopic study of young volcanic rocks from mid-ocean ridges, ocean islands and island arcs: Royal Society of London Philosophical Transactions, ser. A., v. 297, no. 1431, p. 409–445.

Taylor, S.R., and McLennan, S.M., 1985, The continental crust; its composition and evolution: Oxford, U.K., Blackwell Scientific, 312 p.

Thompson, R.N., Morrison, M.A. Hendry, G.L., and Parry, S.J., 1984, An assessment of the relative roles of crust and mantle in magma genesis—an elemental approach: Royal Society of London Philosophical Transactions, ser. A, v. 310, no. 1514, p. 549–590.

Thorpe, R.S., Francis, P.W., and O'Callaghan, L.J., 1984, Relative roles of source composition, fractional crystallization and crustal contamination in the petrogenesis of Andean volcanic rocks: Royal Society of London Philosophical Transactions, ser. A, v. 310, no. 1514, p. 675–692.

Trop, J.M., 1996, Sedimentological, provenance, and structural analysis of the lower Cantwell Formation, Cantwell Basin, central Alaska Range; implications for the development of a thrust-top basin: West Lafayette, Ind., Purdue University, M.S. thesis, 222 p.

Walker, G.P.L., 1971, Grain size characteristics of pyroclastic deposits: Journal of Geology, v. 79, no. 6, p. 696–714.

Wallace, W.K., and Engebretson, D.C., 1984, Relationship between plate motions and Late Cretaceous to Paleogene magmatism in southwestern Alaska: Tectonics, v. 3, no. 2, p. 295–315.

Wilson, F.H., Dover, J.H., Bradley, D.C., Weber, F.R., Bundtzen, T.K., and Haeussler, P.J., 1998, Geologic map of central (interior) Alaska: U.S. Geological Survey Open-File Report 98–133 [CD–ROM].

Wilson, Marjorie, and Davidson, J.P., 1984, The relative roles of crust and upper mantle in the generation of oceanic island arc magmas: Royal Society of London Philosophical Transactions, ser. A, v. 310, no. 1514, p. 661–674.

Wolfe, J.A., and Wahrhaftig, Clyde, 1970, The Cantwell Formation of the central Alaska Range, *in* Changes in stratigraphic nomenclature by the U.S. Geological Survey, 1968: U.S. Geological Survey Bulletin 1294–A, p. A41–A46.

Wright, J.V., Smith, A.L., and Self, Stephen, 1980, A working terminology of pyroclastic deposits: Journal of Volcanology and Geothermal Research, v. 8, no. 2–4, p. 315–336.